Miocene Amazonian biodiversity under the microscope: small erethizontoid and chinchilloid caviomorph rodents from the Solimões Formation in Brazil

EMMANUELLE FONTOURA, LEONARDO KERBER, LAURENT MARIVAUX, PIERRE-OLIVIER ANTOINE, NARLA S. STUTZ, FRANCISCO RICARDO NEGRI, ANA MARIA RIBEIRO, and MYRIAM BOIVIN



Fontoura, E., Kerber, L., Marivaux, L., Antoine, P.-O., Stutz, N.S., Negri, F.R., Ribeiro, A.M., and Boivin, M. 2026. Miocene Amazonian biodiversity under the microscope: small erethizontoid and chinchilloid caviomorph rodents from the Solimões Formation in Brazil. *Acta Palaeontologica Polonica* 71 (4): 717–741.

The caviomorph rodent diversity of the Solimões Formation (Upper Miocene, Brazil) has revealed remarkable taxonomic richness, offering key insights into the evolutionary history of Amazonian biodiversity. However, small caviomorphs, which are likely the most diverse within the clade, remain poorly known, due to difficulties in recovering their fossil remains. This study describes new dental remains of small-sized caviomorphs from the "Coqueiros" fossil-bearing locality (Envira River, State of Acre, Brazil), obtained by wet-screening of the sediments process. The material comprises three new species of Erethizontoidea, assigned to two genera. *Micronoamys* Fontoura gen. nov., represented by *Micronoamys candelae* Fontoura sp. nov., is the smallest known Miocene erethizontoid and shows high-crowned molars, unilateral hypsodonty, a short oblique hypoflexus and a posteroloph initially disconnected from the hypocone area. *Enviramys* Fontoura gen. nov., with *Enviramys vucetichae* Fontoura gen. et sp. nov. and *Enviramys nasifae* Fontoura sp. nov., exhibits small size, brachydonty, and elongated crests and flexi. Additional remains of cf. *Microscleromys* sp. and "*Scleromys*" sp. were also identified. Computed tomography (Micro-CT) was used to evaluate tooth wear patterns and visualize morphological features, allowing for comparisons between wear stages. The presence of small, presumably arboreal erethizontoids suggests forested habitats, consistent with other Miocene sites in Western Amazonia. These findings expand our knowledge of the Miocene rodent diversity in South America, especially in Proto-Amazonia. They also highlight biogeographic connections between Western Amazonian and adjacent Miocene faunas. The discovery of these small-sized rodents emphasizes the importance of wet screening of fossil-bearing sediments in recovering poorly represented taxa and contributes to refining our knowledge of mammalian evolution and biogeography in the Amazonian region.

Key words: Mammalia, Hystricognathi, Late Miocene, Western Amazonia, State of Acre, Envira River, Brazil.

Emmanuelle Fontoura [fontourapaleo@gmail.com; ORCID: https://orcid.org/0000-0002-3907-618X], Museu de Ciências Naturais, Secretaria do Meio Ambiente e Infraestrutura, R. Dr. Salvador França, 1427, 90690-000, Porto Alegre, Rio Grande do Sul, Brazil and Programa de Pós-Graduação em Biodiversidade Animal (PPGBA), Universidade Federal de Santa Maria (UFSM), Av. Roraima, 1000, 97105-900, Santa Maria, Rio Grande do Sul, Brazil.

Leonardo Kerber [leonardokerber@gmail.com; ORCID: https://orcid.org/0000-0001-8139-1493], Programa de Pós-Graduação em Biodiversidade Animal (PPGBA), Universidade Federal de Santa Maria (UFSM), Av. Roraima, 1000, 97105-900, Santa Maria, Rio Grande do Sul, Brazil and CAPPA - Centro de Apoio à Pesquisa Paleontológica da Quarta Colônia, R. Maximiliano Vizzotto, 598, 97230-000, São João do Polêsine, Rio Grande do Sul, Brazil.

Laurent Marivaux [laurent.marivaux@umontpellier.fr; ORCID: https://orcid.org/0000-0002-2882-0874], Pierre-Olivier Antoine [pierre-olivier.antoine@umontpellier.fr; ORCID: https://orcid.org/0000-0001-9122-1818], and Narla S. Stutz [narlasstutz@gmail.com; ORCID: https://orcid.org/0000-0002-1937-3902], Institut des Sciences de l'Évolution de Montpellier (ISEM), Université de Montpellier, CNRS, IRD, Place Eugène Bataillon, 34090, Montpellier, France.

Francisco Ricardo Negri [frnegriufac@gmail.com; ORCID: https://orcid.org/0000-0001-7396-0334], Universidade Federal do Acre (UFAC), Campus Floresta, Estrada do Canela Fina, Km 12, 69980-000, Cruzeiro do Sul, Acre, Brazil.

Ana Maria Ribeiro [ana-ribeiro@sema.rs.gov.br; ORCID: https://orcid.org/0000-0003-4167-8558], Museu de Ciências Naturais, Secretaria do Meio Ambiente Infraestrutura (SEMA), R. Dr. Salvador França, 1427, 90690-000, Porto Alegre, Rio Grande do Sul, Brazil and Programa de Pós-Graduação em Sistemática e Conservação da Diversidade Biológica, SEMA and UERGS, Rua Dr. Salvador França, 1427, 90690-000, Porto Alegre, Rio Grande do Sul, Brazil.

Myriam Boivin [mboivin@idgym.unju.edu.ar; ORCID: https://orcid.org/0000-0002-5240-9460], Grupo de Paleontología de Vertebrados, Instituto de Ecorregiones Andinas (INECOA), Universidad Nacional de Jujuy (UNJu), CONICET, Av. Bolivia, 1661, 4600, San Salvador de Jujuy, Jujuy, Argentina and Instituto de Geología y Minería, UNJu, Av. Bolivia, 1661, 4600, San Salvador de Jujuy, Jujuy, Argentina.

Received 8 April 2026, accepted 20 July 2026, published online 19 November 2026.

Copyright © 2026 E. Fontoura et al. This is an open-access article distributed under the terms of the Creative Commons Attribution License (for details please see http://creativecommons.org/licenses/by/4.0/), which permits unrestricted use, distribution, and reproduction in any medium, provided the original author and source are credited.

Introduction

Caviomorpha is a clade of hystricognathous rodents, endemic to the Neotropics, exhibiting remarkable taxonomic, morphological, and ecological diversity (e.g., Patton et al. 2015; Wilson et al. 2016; Álvarez et al. 2017; Robinet et al. 2020, 2022, 2025; Mammal Diversity Database 2025). The evolutionary history of this group is evident in its rich fossil record, beginning with its first appearance in Peruvian Amazonia at the end of the Eocene, followed by rapid diversification before the end of Oligocene (e.g., Antoine et al. 2012; Bertrand et al. 2012; Vucetich et al. 2015; Boivin et al. 2017a,b, 2018, 2019, 2022; Kerber 2017; Assemat et al. 2019; Arnal et al. 2020, 2022; Marivaux et al. 2020; Buffan et al. 2025; Stutz et al. 2026). Extant caviomorphs are divided into two major molecular-based clades, Erethicavioi Boivin in Boivin et al., 2019 and Octochinchilloi Boivin in Boivin et al., 2019. These clades include four less inclusive clades (=superfamilies): Cavioidea Fischer de Waldheim, 1817 (e.g., guinea pigs and related forms), Erethizontoidea Bonaparte, 1845 (New World porcupines), Chinchilloidea Bennett, 1833 (chinchillas and pacaranas), and Octodontoidea Waterhouse, 1839 (e.g., spine rats, nutrias, and related forms) (e.g., Rowe and Honeycutt 2002; Woods and Kilpatrick 2005; Upham and Patterson 2012, 2015; Verzi et al. 2013, 2015, 2016; Voss et al. 2013; Arnal and Vucetich 2014; Kerber et al. 2017c, 2018a, b; Rasia and Candela 2019; Rasia et al. 2021).

The Miocene outcrops of South America have yielded an extensive record of caviomorphs, encompassing a wide taxonomic diversity. At mid and high latitudes, caviomorph faunas were discovered in Argentina (e.g., Cerro Azul, Collon Curá, Ituzaingó, Pinturas, Santa Cruz, and Sarmiento formations; Vucetich et al. 1993, 2010b, 2015; Vucetich and Kramarz 2003; Kramarz and Bellosi 2005; Candela and Nasif 2006; Nasif et al. 2013; Esteban et al. 2014; Deschamps and Tomassini 2016; Arnal et al. 2019; Piñero et al. 2021a), Bolivia (e.g., Quebrada Honda; Croft et al. 2011), Chile (e.g., Pampa Castillo and Laguna del Laja; Flynn et al. 2002, 2008; Solórzano et al. 2021; McGrath et al. 2022, 2023), and Uruguay (Camacho Formation; e.g., Rinderknecht et al. 2017; Perea et al. 2023). At low latitudes, the fossil record is also extensive in terms of proportional geographic area, including several well-sampled and more recently documented localities, occurring in Brazil (Solimões Formation, several localities, including Niterói, Talismã, Patos, Cachoeira do Bandeira, "Coqueiros"; e.g., Sant'Anna-Filho 1994; Negri and Ferigolo 1999; Kerber et al. 2017c; Fontoura et al. 2023, 2024), Colombia (La Venta, Honda Group; e.g., Fields 1957; Walton 1990, 1997; Carrillo et al. 2023), Ecuador (Anthony 1922), Peru (e.g., Contamana, Fitzcarrald, Madre de Dios, Tarapoto [TAR-31]; Antoine et al. 2007, 2013, 2016; Tejada-Lara et al. 2015; Boivin et al. 2021), and Venezuela (e.g., Socorro Formation; Carrillo and Sánchez-Villagra 2015; Carrillo-Briceño et al. 2021). Although this region has been comparatively less studied, both temporally and quantitatively, it nonetheless exhibits a broad taxonomic diversity.

The Solimões Formation (Upper Miocene), situated in the Acre Basin, western Brazil, has yielded a considerable array of vertebrate fossils since the 19th century (Chandless Expedition [Chandless 1866], see also Agassiz and Agassiz 1868; Cozzuol 2006; Latrubesse et al. 2007; Hsiou et al. 2022; Stutz et al. 2023; Marivaux et al. 2023), with a particular diversity and abundance of caviomorphs (see Kerber et al. 2017c). Nevertheless, small rodents, such as octodontoids and erethizontoids, along with other small mammals, are less commonly represented (e.g., Campbell et al. 2006; Kerber 2017; Kerber et al. 2017c). This does not necessarily indicate a true absence of individuals, but rather a bias regarding preservation and collection (Walton 1997). Studies of caviomorphs from the Solimões Formation in Brazil were initiated in the second half of the 20th century by Patterson (1942), followed by Paula-Couto (1978, 1983), Frailey (1986), and Mones and Toledo (1989). In the 1990s, rodents were studied by Sant'Anna-Filho (1994), Bergqvist et al. (1998), and Negri and Ferigolo (1999). Since the 21st century, fossil caviomorph studies have been published by Campbell et al. (2006) and Kerber et al. (2016, 2017a, c; see Kerber 2017 for more details). A new rodent fauna was recently reported from the Solimões Formation, in Upper Miocene deposits at the "Coqueiros" locality (PRE06, Fig. 1), located on the right bank of the Envira River in State of Acre, encompassing octodontoids, dinomyids, chinchilloids, and cavioids (Fontoura et al. 2023, 2024). The Envira River, a meandering river that experiences annual flooding, exposes fossil-bearing layers of the Solimões Formation during dry seasons. Although these layers have not been dated by radiometric methods yet, two other localities from the Solimões Formation, Niterói and Talismã, have been dated using detrital zircons, which indicated maximum ages between 10.89 and 8.5 million years ago, supporting at most a Tortonian age for the formation (Bissaro-Júnior et al. 2019). Additionally, the fossil assemblage from "Coqueiros" suggests a Late Miocene biostratigraphic age (Chasicoan South American Land Mammal Age—SALMA; see Fontoura et al. 2023).

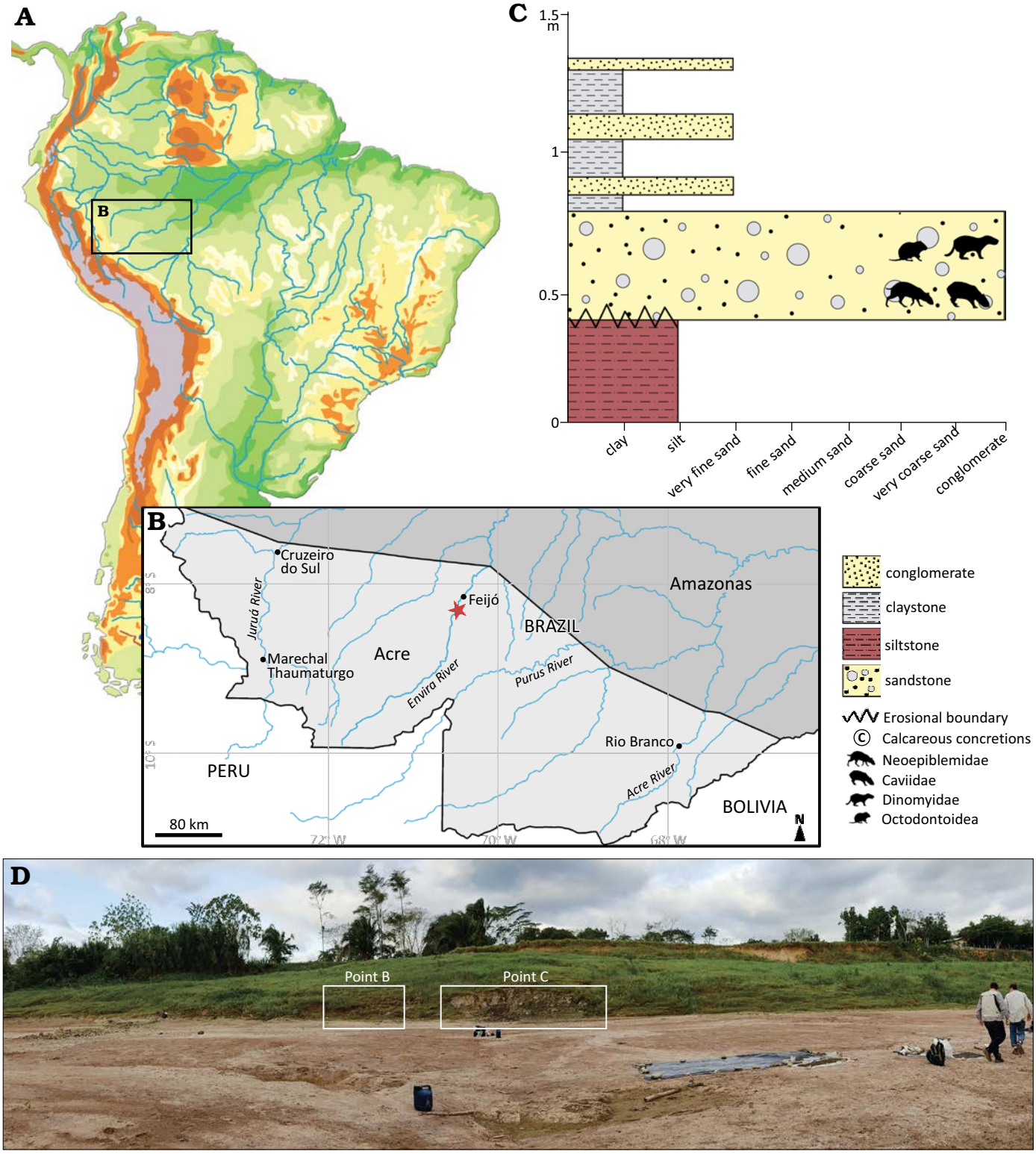


Fig. 1. **A**. Location of the study area within South America. **B**. Map of the State of Acre (Brazil) showing the location of the PRE06 "Coqueiros" fossil-bearing locality on the right bank of the Envira River (red star; modified from Fontoura et al. 2024). **C**. Stratigraphic section of the Solimões Formation at "Point B" from Outcrop PRE06 (modified from Stutz et al. 2023). **D**. Photo of the fossil-bearing locality and collection points (points B and C).

Tooth wear represents a significant challenge in paleontology, as it often leads to the loss of crucial morphological details essential for accurate taxonomic identification of species (e.g., Koenigswald 2016). The advent of computed tomography has revolutionized the way we study hidden structures, enabling the analysis of 3D objects without causing any damage to the specimen.

The goal of this study is to further our understanding of

the diverse Amazonian fossil record by (i) describing newly discovered isolated dental specimens attributed to Miocene erethizontoids and chinchilloids from the PRE06 locality on the Envira River, State of Acre, Brazil; and (ii) exploring the biogeographic implications of these findings.

Nomenclatural acts.—This published work and the nomenclatural acts it contains have been registered in ZooBank: urn:lsid:zoobank.org:pub:26ABF0B7-2C15-4BC7-977B-7468AB83AC72.

Institutional abbreviations.—MACN, Museo Argentino de Ciencias Naturales "Bernardino Rivadavia", Buenos Aires, Argentina; MLP, Museo de La Plata, La Plata, Argentina; UFAC, Universidade Federal do Acre, Rio Branco, Brazil; UFAC-CS, Universidade Federal do Acre—Campus Floresta, Cruzeiro do Sul, Brazil; JUY, Universidad Nacional de Jujuy, San Salvador de Jujuy, Argentina; MUSM, Museo de Historia Natural de la Universidad Nacional Mayor San Marcos, Lima, Peru.

Other abbreviations.—Hb, maximum labial crown height; Hg, maximum lingual crown height; HI, hypsodonty index; mdl, maximum mesiodistal length; mw, maximum width. We follow standard convention in abbreviating tooth families as I, C, P, and M, with upper and lower case letters referring to upper and lower teeth, respectively.

Material and methods

Paleontological overview of the Solimões Formation.—The Solimões Formation is notable for its extensive vertebrate fossil record, which includes a diverse array of mammals through several fossil-bearing localities. These fossils document the occurrence of bats, cetaceans, litopterns, marsupials, notoungulates, primates, rodents, sirenians, and xenarthrans (e.g., Frailey 1986; Kay and Frailey 1993; Sant'Anna 1994; Campbell et al. 2006; Kay and Cozzuol 2006; Negri et al. 2010; Ribeiro et al. 2013; Kerber et al. 2016, 2017a, c, 2018a, b; Fontoura et al. 2023, 2024; Stutz et al. 2023). In addition, fossils of birds, crocodilians, chelonians, fish, amphibians, invertebrates, ichnofossils, and plants have been identified (e.g., Cozzuol 2006; Negri et al. 2010; Silva and Negri 2016; Souza-Filho et al. 2020; Muniz et al. 2021, 2022). Recent dating of fossiliferous localities from this formation indicates maximum ages of deposition in the Tortonian, corresponding to the Late Miocene (Bissaro-Júnior et al. 2019).

Collection.—The specimens analyzed in this study were collected at the Ponto Rio Envira 06 (PRE06 Outcrop; 08°18'12.6" S and 70°26'39.9" W; Fig. 1), also called "Coqueiros", Envira River, Feijó Municipality, State of Acre, Brazil. Field expeditions took place in 2010, 2019, 2022, and 2024. We excavated and collected the sediment of two levels at this locality (Fig. 1: points B and C; see Stutz et al. 2023; Fontoura et al. 2024 for specific details), which belong to the same stratigraphic horizon. The fossil-bearing layers consist of one ~50 cm-thick ("Point B") and one ~10 cm-thick ("Point C") slightly indurated conglomerate, composed of carbonate concretions and fossil fragments (currently under study). The sediments were processed by wet screening with sieves of 2 mm, 1 mm, and 0.6 mm meshes, applied sequentially in situ with the water of the Envira River. The fossil remains were then extracted from the residues of screening at the Paleontology Laboratory of the Universidade Federal do Acre (Cruzeiro do Sul, State of Acre, Brazil) and the Paleontology Section of the Museu de Ciências Naturais, Secretaria do Meio Ambiente e Infraestrutura (Porto Alegre, Rio Grande do Sul, Brazil). The specimens were sorted by picking under stereomicroscopes and cleaning by with ultrasonic and manual methods. They are curated in the Paleontology Laboratory collection, Universidade Federal do Acre, Floresta Campus, State of Acre, Brazil (UFAC-CS).

Comparisons and nomenclature.—The specimens were described and compared with bibliographic sources on extinct and extant octodontoids (e.g., Walton 1990, 1997; Kramarz and Bellosi 2005; Antoine et al. 2007; Vucetich et al. 2010b, 2015; Croft et al. 2011; Arnal and Pérez 2013; Verzi et al. 2016; Candela et al. 2021; Piñero et al. 2021b), erethizontoids (e.g., Candela 2002, 2004; Candela et al. 2021; Ercoli et al. 2021), and chinchilloids (e.g., Kerber et al. 2016; Rasia and Candela 2019; Boivin et al. 2021; Candela et al. 2021). We followed Boivin and Marivaux (2020, and the literature cited therein) and Boivin et al. (2021) for dental nomenclature; and Candela (1999), for additional dental nomenclature of Erethizontoidea. We followed the phylogenetic analyses performed by Boivin et al. (2019). Lower-case or upper-case letters were used for lower dentitions (dp, for lower deciduous premolar; m, for lower molars; dP, for upper deciduous premolar; and M, for upper molars). We standardized the nomenclature for dental connections, with the term "strongly connected" referring to cases where dentine is visible in the connection, and as thick as the enamel, while "slightly connected" is used when only the enamel is visible.

Analysis and dental associations.—The challenge of using isolated teeth for taxonomic identification lies in the understanding of morphological variation, which can be classified into four categories: (i) inter-specific or inter-taxonomic; (ii) polymorphism; (iii) occlusal tooth wear; and (iv) the position of each tooth (dental locus; Calandra et al. 2016; Boivin et al. 2021; Vitek and Chen 2022). It thus becomes necessary to establish criteria for organizing the aforementioned variation. The criteria used to determine the locus of the isolated teeth and taxonomically associate them to the mandible and maxilla are an adaptation of those proposed by Boivin et al. (2021). These criteria include the following: (i) similar size; (ii) similar crown height; (iii) presence and/or absence of mesial/distal contact facets (to distinguish (d)p4/(d)P4, which has only distal contact facet, from m1/M1 or m2/M2, having both contact facets, and from m3/M3, with only the mesial contact facet); (iv) similar occlusal pattern (for fur-

ther details, see descriptions in the Systematic palaeontology section); and (v) similar tooth wear (with the support of computed tomography methodology, see below). In cases where uncertainty existed regarding the determination of the loci, the designation "locus uncertainty" was used and labelled with a question mark (e.g., dp4?, m1?, m2?, and m3?).

The measurements were obtained using the Image J software (Schroeder et al. 2021; version 1.54g): the maximum mesiodistal length (mdl), the maximum width (mw), the maximum labial crown height (Hb) and maximum lingual crown height (Hg). The hypsodonty index (HI) of a tooth follows the method proposed by Janis (1986) and is calculated as the maximum crown height divided by the mesiodistal length (H/mdl). Teeth with an HI < 1 are considered brachydont, those with an HI = 1 are mesodont, and those with an HI > 1 are hypsodont (Janis 1986). As no specific index exists for upper molars exhibiting unilateral hypsodonty, we opted to apply the framework of Janis (1986) as the most suitable available reference. It is important to note that, alongside the brachydont condition, hypsodont teeth include subcategories such as protohypsodont (with roots, as seen here) and euhypsodont (without roots).

Dental wear assessment and morphological variations.—To enhance the visualization of morphological structures, enabling more accurate taxonomic identification, particularly in small specimens, computed tomography (Micro-CT) was employed. Some of the specimens were scanned (UFAC-CS 190, 205, 247, 252, 253, 255, and 259), with a resolution of 7.1 μm, using a high-energy μCT-scanning station SkyScan1173 from the technical facilities of the Instituto de Petróleo e dos Recursos Naturais, Pontifícia Universidade Católica do Rio Grande do Sul, Brazil. The raw scan data were exported from the scanner computer in TIFF format. Segmentation and 3D surface rendering were performed using 3D Slicer software (Fedorov et al. 2012; version 4.11).

Furthermore, virtual reconstructions generated from CT scans allowed the estimation of occlusal tooth wear and the digital standardization of specimens across different wear stages. This approach enabled the comparison of occlusal dental morphology under different wear scenarios and among specimens at various ontogenetic stages (Skandalos and van den Hoek Ostende 2023; Fontoura et al. 2024). This technique is of critical importance in paleontology, as the preservation of fossils representing all life stages is rare. As an example of the applicability of this approach, this methodology was applied by Skandalos and van den Hoek Ostende (2023), resulting in the synonymization of species (e.g., *Pliospalax sotirisi* as a junior synonym of *P. macoveii*).

In this context, to visualize the morphological modifications in enamel and dentine resulting from occlusal tooth wear, the 3D Slicer software (Fedorov et al. 2012) was employed, adapting the methodology of Skandalos and van den Ostende (2023). The methodology consists of creating cross-sections for each tooth, parallel to the occlusal axis, with a spacing of seven to ten slices between each crosscut, simulating the tooth wear of the teeth (Koenigswald 2016). Each isolated tooth scanned here generated between one and 15 wear stages, with some of the most relevant stages selected for discussion below.

It is important to emphasize that, in some specimens (UFAC-CS 247, 252, 253, 255, 259, 375, and 402), occlusal tooth wear was documented using two complementary approaches: (i) a simulated reconstruction, consisting of the estimated wear progression described above, derived from a single specimen (i.e., UFAC-CS 247 and 253) through computed tomography; and (ii) an empirical representation based on specimens exhibiting different wear stages, reflecting intraspecific variation. Both approaches are complementary within a taxonomic framework. Throughout the text, whenever variation associated with tooth wear progression is discussed, the corresponding plates illustrating either the empirical or the simulated variation are explicitly indicated.

Systematic palaeontology

Rodentia Bowdich, 1821

Hystricognathi Tullberg, 1899

Caviomorpha Wood & Patterson in Wood, 1955

Erethicavioi Boivin in Boivin, Marivaux, and Antoine, 2019

Erethizontoidea Bonaparte, 1845

Genus *Micronoamys* Fontoura nov.

ZooBank LSID: urn:lsid:zoobank.org:act:64966C6C-4C4C-48E5-9093-807471CCF9DF.

Type species: *Micronoamys candelae* Fontoura gen. et sp. nov., monotypic, see below.

Etymology: A combination of the Greek *micro-* (μικρός), small, with *noamys*, referencing the similar morphology to the genus *Noamys* Ercoli et al., 2021. Therefore, *Micronoamys* denotes a smaller form resembling *Noamys*.

Diagnosis.—As for the type and only species.

Micronoamys candelae Fontoura sp. nov.

Figs. 2A–D, 3.

ZooBank LSID: urn:lsid:zoobank.org:act:2C939E14-88D2-4501-8BC5-77D06348EAB5.

Etymology: In honor of Adriana M. Candela (División Paleontología Vertebrados, Museo de La Plata, Buenos Aires, Argentina) in recognition of her outstanding contributions to the study of South American fossil rodents, particularly in systematics, evolution, and paleobiogeography of erethizontoids.

Holotype: UFAC-CS 247, left M1 or M2 (Fig. 2A).

Type locality: PRE06 locality, "Coqueiros" (08°18'12.6"S, 70°26'39.9"W), Envira River, Feijó Municipality, State of Acre, Brazil, Western Amazonia.

Type horizon: Solimões Formation, Upper Miocene (see Fontoura et al. 2023).

Diagnosis.—Small rodent displaying cheek teeth with non-taeniodont pattern; tetralophodont upper molars with thick enamel. Upper molars with: mesiodistally elongated shape

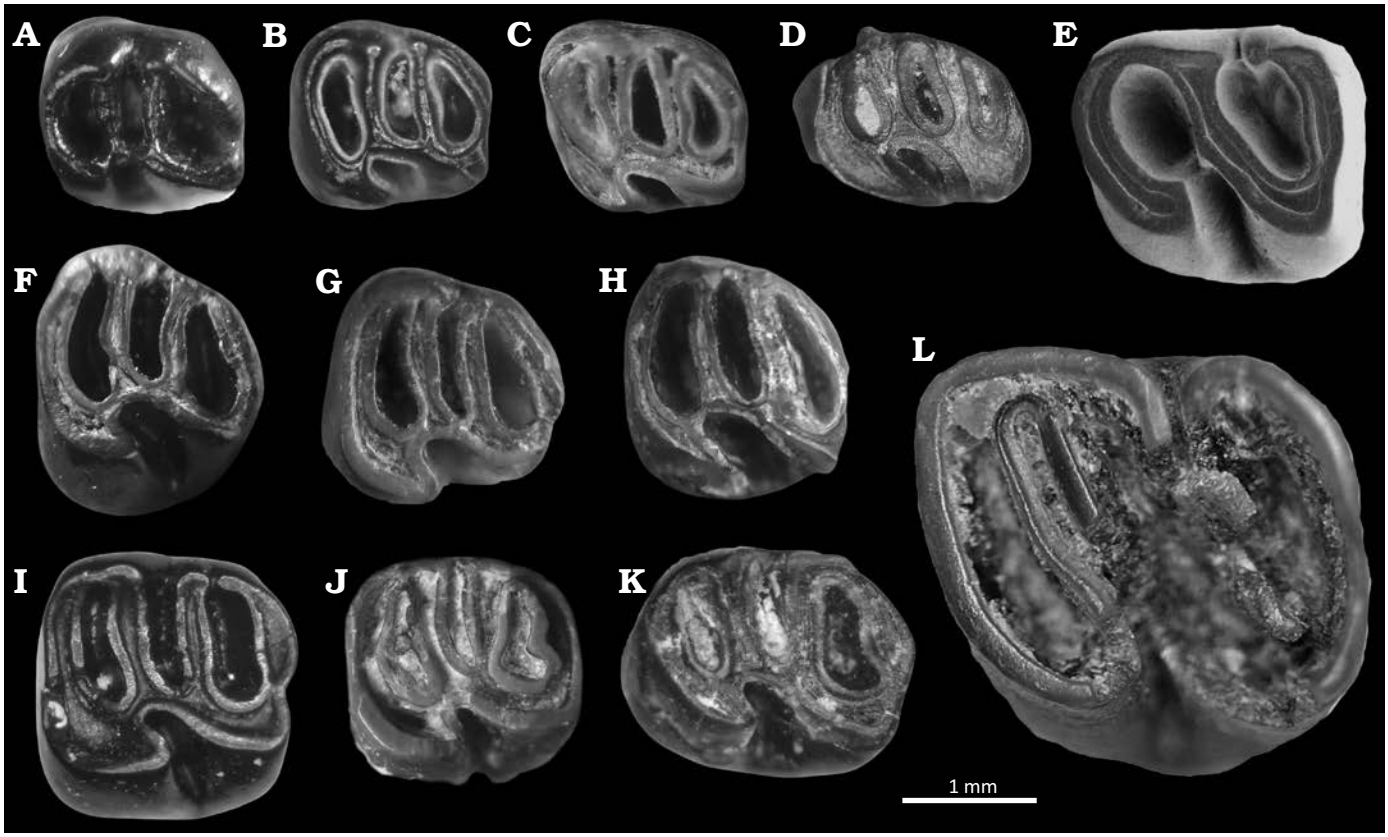


Fig. 2. Erethizontoid and chinchilloid rodents from PRE06 locality, Brazil (Upper Miocene), teeth in occlusal view. **A**–**D**. *Micronoamys candelae* Fontoura gen. et sp. nov. **A**. UFAC-CS 247, holotype, M1 or M2. **B**. UFAC-CS 402, M2? (reversed). **C**. UFAC-CS 255, M2? (reversed). **D**. UFAC-CS 375, M? (reversed). **E**. cf. *Microscleromys* sp.; UFAC-CS 190, m1 or m2. **F**–**H**. *Enviramys vucetichae* Fontoura gen. et sp. nov. **F**. UFAC-CS 253, holotype, M3 (reversed). **G**. UFAC-CS 259, M3? (reversed). **H**. UFAC-CS 252, M? (reversed). **I**–**K**. *Enviramys nasifae* Fontoura gen. et sp. nov. **I**. UFAC-CS 449, holotype, M1 or M2 (reversed). **J**. UFAC-CS 404, M1 or M2 (reversed). **K**. UFAC-CS 446, dP4. **L**. "*Scleromys*" sp.; UFAC-CS 205, m1 or m2?.

and an oval to trapezoidal outline; unilateral hypsodonty; straight, transverse or slightly oblique crests, roughly parallel between them; prominent labial cusps; parafossette, mesoflexus, and metafossette + posterofossette with a subtriangular to oval shape, which could be notably broader in the mesiodistally dimension; hypoflexus highly oblique (in occlusal view), mesially oriented, and notably short linguolabially; wide and usually long mure, slightly oblique or almost parallel to the sagittal plane; second crest (protoloph) formed by a single crest; mesiodistal enlargement situated labially to/on the posteroloph interpreted as metacone; posteroloph relatively short, disconnected from the posterior arm of hypocone in early stages of wear; long posterior arm of hypocone; paracone and mesostyle at the same labiolingual level in occlusal view (paracone slightly higher in labial view) and strongly connected to the anteroloph and the posteroloph/?metacone, respectively; short posterior outgrowth of protocone; posterior arm of the protocone weakly reaching the mure and the protoloph in early stages of wear.

Material.—Holotype and UFAC-CS 255, left M2? (Fig. 2C); UFAC-CS 375, right upper molar (Fig. 2D); UFAC-CS 402, right M2? (Fig. 2B) from the type locality and horizon.

Description.—The new specimens were found in the same stratigraphic level and are considered to be a single species due to their compatible size and similar general molar morphology. These teeth are from a small-sized erethizontoid, especially by their non-taeniodonty, extended flexi, and weak obliquity of lophs (Boivin et al. 2021), with the maximum mesiodistal length between 1.57 and 1.79 mm, and a maximum linguolabially width between 1.38 and 1.56 mm (Table 1). These measurements indicate that this taxon is the smallest known Miocene erethizontoid, even smaller than the Middle Miocene *Nuyuyomys chinqaska* Boivin & Walton in Boivin et al., 2021 (upper molars with average dimensions of 2.21 mm mesiodistally and 2.25 mm linguolabially; Boivin et al. 2021); the late Middle Miocene *Microsteiromys jacobsi* Boivin & Walton in Boivin et al., 2021 (dp4, 2.66 mm mesiodistally and 2.33 mm linguolabially; lower molars with average of 3.06 mm mesiodistally and 2.4 mm linguolabially; upper molars are unknown; Boivin et al. 2021); the Middle Miocene cf. *Microsteiromys* sp. (P4, 2.14 mm mesiodistally and 2.20 mm linguolabially; M3? with average of 2.44 mm mesiodistally and 2.11 mm linguolabially; Antoine et al. 2013); and the Late Miocene–early Pliocene *Noamys hypsodonta* Ercoli et al., 2021 (dP4, 3.16 mm mesiodistally and 2.5 mm linguolabially; M1, 3.14 mm mesiodistally and 2.65 mm linguolabially; measurements taken directly from the original

Table 1. List of specimens from PRE06, Rio Envira, State of Acre, Brazil, respective dental position, and measurements (in mm). Abbreviations: Hb, maximum labial crown height; Hg, maximum lingual crown height; HI, hypsodonty index; mdl, mesiodistal length; mw, the maximum width; * fragmented and heavily worn tooth.

Specimens	Taxon	Dental position	mdl	mw	Hb	Hg	HI
UFAC-CS 190	cf. *Microscleromys* sp.	right m1 or m2	2.26	1.98	1.30	1.01	0.58
UFAC-CS 205	"*Scleromys*" sp.	right m1 or m2?	3.3	2.94	~4.54	~4.16	1.38
UFAC-CS 247	*Micronoamys candelae* Fontoura gen. et sp. nov.	left M1 or M2	1.57	1.38	0.85	1.88	1.20
UFAC-CS 252	*Enviramys vucetichae* Fontoura gen. et sp. nov.	right M?	1.7	1.52	0.89	1.34	0.79
UFAC-CS 253	*Enviramys vucetichae* Fontoura gen. et sp. nov.	right M3	1.55	1.72	0.80	1.27	0.82
UFAC-CS 255	*Micronoamys candelae* Fontoura gen. et sp. nov.	left M2?	1.79	1.56	0.62	1.53	0.85
UFAC-CS 259	*Enviramys vucetichae* Fontoura gen. et sp. nov.	right M3?	1.71	1.79	0.77	1.25	0.73
UFAC-CS 375	*Micronoamys candelae* Fontoura gen. et sp. nov.	right M*	1.78	1.39	0.56	0.99	0.56
UFAC-CS 402	*Micronoamys candelae* Fontoura gen. et sp. nov.	right M2?	1.58	1.5	0.60	1.39	0.88
UFAC-CS 404	*Enviramys nasifae* Fontoura gen. et sp. nov.	right M1 or M2	1.86	1.58	0.65	1.10	0.59
UFAC-CS 446	*Enviramys nasifae* Fontoura gen. et sp. nov.	left dP4	1.78	1.36	0.70	1.45	0.81
UFAC-CS 449	*Enviramys nasifae* Fontoura gen. et sp. nov.	right M1 or M2	1.84	1.7	0.64	1.21	0.66

specimen to standardize comparison). Also, it is smaller than Oligocene taxa originally described as erethizontoids (see Boivin et al. 2019): *Shapajamys labocensis* Boivin et al., 2018 (upper molars with average dimensions of 2.18 mm mesiodistally and 2.28 mm linguolabially; Boivin et al. 2018) and *Palaeosteiromys amazonensis* Boivin in Boivin et al., 2017a (upper molars with 2.16 mm mesiodistally and 2.2 mm linguolabially; Boivin et al. 2017a).

All specimens are upper teeth. This assumption is based on the root morphology (presence of three roots: one more elongated mesiodistally in the lingual region, and two more circular in the labial region). UFAC-CS 375 is heavily worn both occlusally and laterally, preventing the visualization of the contact facets. Thus, we cautiously assign it as an upper molar. The other specimens (UFAC-CS 247, 255, 402) have both contact facets. In UFAC-CS 247, this feature is very subtle, as it represents a recently erupted tooth. It has tetralophodont pattern in upper molars (Fig. 2A–D), similar to *Noamys hypsodonta* (Ercoli et al. 2021), and different from *Nuyuyomys chinqaska* (Boivin et al. 2021) and *Palaeosteiromys amazonensis* (Boivin et al. 2018). Upper molars are non-taeniodont, similar to several erethizontoids and different from *Eosteiromys annectens* (Ameghino, 1899) (Kramarz 2004). The upper molars are more elongated mesiodistally than linguolabially. They have an oval, as in *Noamys hypsodonta*, to trapezoidal shape. The labial margin is strongly curved. The labial cusps are well marked, except the metacone. The crests are straight or slightly oblique and parallel. Considering the maximum crown height, the HI ranges from 1.20 (UFAC-CS 247) to 0.88 (UFAC-CS 402). This range variation is attributed to differences in the wear stage of the specimens, as UFAC-CS 247 shows only minimal wear (Fig. 2A), while UFAC-CS 402 exhibits advanced wear (Fig. 2B). The specimen UFAC-CS 375 presents extensive wear (Fig. 2D), which precluded accurate measurements of crown height. So, this species is classified as protohypsodont, a category different from the common pattern of erethizontoids, but similar to *Noamys hypsodonta* (HI = 1.09). Particularly, unilateral hypsodonty is observed on UFAC-CS 247, with the lingual region higher than the labial one (0.85 mm labially vs. 1.88 mm lingually; Fig. 3A_7–A_9), as in *Noamys hypsodonta* (mean crown height of dP4 and M1: 1.67 mm labially vs. 3.35 mm lingually).

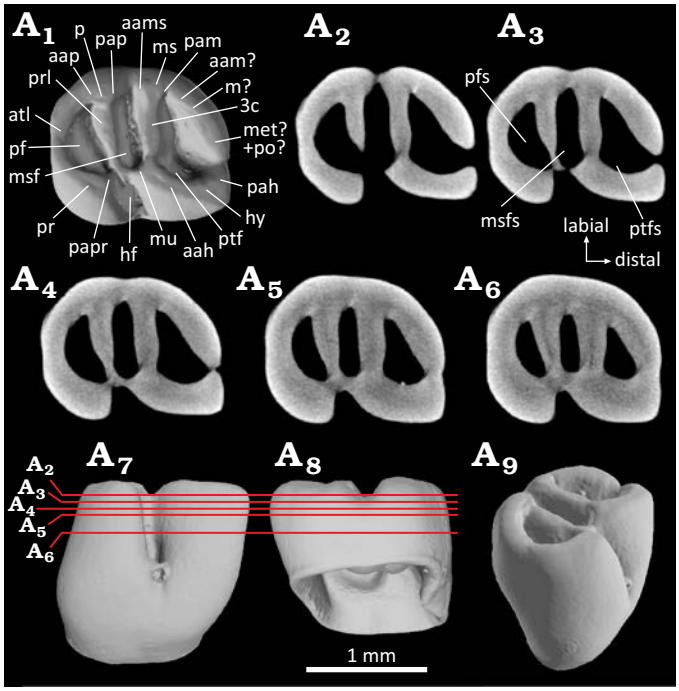


Fig. 3. Three-dimensional reconstruction of the erethizontoid rodent *Micronoamys candelae* Fontoura gen. et sp. nov., holotype M1 or M2 (UFAC-CS 247) from PRE06 locality, State of Acre, Brazil (Upper Miocene). Tooth in occlusal (A_1), lingual (A_7), labial (A_8), and oblique mesiolabial (A_9) views, estimate of tooth wear (A_2–A_6), the position of slices indicated in A_7, A_8. Abbreviations: aah, anterior arm of the hypocone; aams, anterior arm of the mesostyle; aap, anterior arm of the paracone; atl, anteroloph; hf, hypoflexus; hy, hypocone; m, metacone; met, metaloph; mu, mure; ms, mesostyle; msf, mesoflexus; msfs, mesofossette; p, paracone; pah, posterior arm of the hypocone; pam, posterior arm of the mesostyle; pap, posterior arm of the paracone; papr, posterior arm of the protocone; pf, paraflexus; pfs, parafossette; po, posteroloph; pr, protocone; prl, protoloph; ptf, posteroflexus + metaflexus; ptfs, posterofossette + metafossette; 3C, third crest.

Mesially, the anteroloph is elongated and oblique in its lingual part and curved distally in its labial part (Figs. 2A–C, 3). On the labial margin, its is oriented toward the paracone, and remains strongly connected to the latter cusp from the time of eruption, as observed on UFAC-CS 247 and in *Noamys hypsodonta*. Distolingually, the protocone exhibits a short posterior outgrowth oriented distally, becoming more evident as dental wear progresses (see Fig. 2A–D). Distolabially there is the posterior arm of the protocone, reaching both the mure and the protoloph in early stages of wear. The protoloph is slightly oblique, as in *Noamys hypsodonta*, and is formed by a single crest. On the labial margin, the protoloph connects to the paracone, which is the largest cusp and slightly higher than the mesostyle in labial view (see UFAC-CS 247, Fig. 2A and *Noamys hypsodonta*).

The mure is broad, straight, and long in UFAC-CS 255, 375, and 402 (Fig. 2B–D), whereas it is slightly oblique in UFAC-CS 255, 402, or almost parallel to the sagittal plane in UFAC-CS 247 (Fig. 2A). The third crest is transverse (UFAC-CS 247, Figs. 2A, 3), or slightly oblique mesiolabially-distolingually (UFAC-CS 255, 375, 402, Fig. 2B–D). This crest may correspond to the mesoloph or the mesoloph + mesolophule, due to a variation in thickness in its medial region. On the labial margin, a mesostyle is visible. The mesostyle and paracone are separated by a shallow notch, closing as wear progresses. The posteroloph is quite robust, relatively short, and slightly oblique. The metacone is indistinguishable, but a structure on the posteroloph, showing a mesiodistal widening as dental wear progresses, could correspond to it. There is a strong connection between the mesostyle and the posteroloph which may represent the anterior arm of the metacone. The metaloph does not appear to be present (= indistinct, as in *Noamys hypsodonta*; Ercoli et al. 2021); however, due to the thickness of the posteroloph, the possibility of its fusion with this crest cannot be ruled out. When newly erupted (as in UFAC-CS 247), the posteroloph is unconnected to the hypocone region, separated from it by a large and deep notch, being apparently the last connection to be closed (with the exception of the hypoflexus; Fig. $3A_4$). Due to the wear, these two structures become strongly connected via a long posterior arm of the hypocone (as in UFAC-CS 255, 375, 402, Fig. 2B–D). With wear, UFAC-CS 247 (Fig. $3A_4$) resembles the condition observed in UFAC-CS 449 (*Enviramys nasifae* Fontoura gen. et sp. nov; Fig. 2I); however, the posterior arm of the hypocone appears to be wider than in *E. nasifae* Fontoura gen. et sp. nov. The hypocone is smaller than the protocone and is located slightly labially (it is aligned, as in UFAC-CS 247; Fig. 3) in relation to the protocone in the horizontal plane (Fig. 3). This is seen in species of *Hypsosteiromys*, *Noamys*, *Parasteiromys*, and *Protosteiromys* (Ercoli et al. 2021). The anterior arm of the hypocone can be in continuity with the mure (UFAC-CS 402 and 255). It is particularly elongated toward the third crest, with its orientation varying, being mesiolabially directed (as in UFAC-CS 375, Fig. 2D) or almost parallel to the sagittal plane (as in UFAC-CS 247, Figs. 2A, 3). Thus, this characteristic may exhibit variation depending on the degree of wear (see Fig. $3A_2$–A_6).

The labial flexi are subtriangular or oval shaped in almost all specimens and are usually extensive mesiodistally, as observed in *Noamys hypsodonta* (Ercoli et al. 2021) and *Marisela gregoriana* Vucetich et al., 2010a (M1–M2; Vucetich et al. 2010a), but unlike the flexus conditions observed in some octodontoids. Uusually the mesoflexus is the largest flexus in octodontoids, e.g., *Acarechimys* (*A. minutes*, DP4–M3 and *A. constans*, DP4–M2; Arnal et al. 2017; McGrath et al. 2023), *Acaremys* (*A. murinus*, DP4–M2; Arnal and Vucetich 2014), *Cercomys* (*C. primitive*, DP4–M3; Montalvo et al. 2019), *Galileomys* (*G. antelucanus*, P4–M3; Vucetich and Kramarz 2003), *Metacaremys* (*M. dimi*, DP4–M2; *M. primitive*, DP4–M3; *M. calfucalel*, DP4–M3; Piñero et al. 2021b) *Caviocricetus* (*C. guenekko*, DP4–M1; McGrath et al. 2023), *Dudumus* (*D. berggreni*, M1–M2; McGrath et al. 2023), and *Prospaniomys* (cf. *P. priscus*, DP4–M3; Arnal and Kramarz 2011). UFAC-CS 247 (Fig. 2A), the parafossette and metafossette + posterofossette are notably larger in the both mesiodistally and labiolingually than the mesoflexus. UFAC-CS 402 (Fig. 2B) and UFAC-CS 255 (Fig. 2C), the mesofossette is mesiodistally longer compared to the two other labial fossettes than in UFAC-CS 247. UFAC-CS 402 and 255, the mesofossette and the posterofossette + metafossette exhibit similar linguolabial extension, with their lingual margin being longer than their labial margin, and with a triangular to oval shape. UFAC-CS 375 (Fig. 2D) could not be evaluated for this parameter due to its advanced stage of dental wear.

The posterofossette + metafossette exhibit a more pronounced length difference between its labial and lingual margins in UFAC-CS 247 (Figs. 2A, 3). The lingual margin of the posterofossette + metafossette is positioned lingual to the mure in the mesiodistal axis in newly erupted teeth (UFAC-CS 247), and it shifts labially as wear progresses, becoming aligned to the mure (as well as to the anterior arm of the hypocone) (UFAC-CS 255, 402). The hypoflexus is narrow linguolabially, and becomes progressively broadened as dental wear advances (Fig. $3A_2$–A_6). In UFAC-CS 402 and 255 (Figs. 2B, C), this flexus is highly oblique with a mesial orientation. The hypostria is deep. The hypoflexus is very oblique and short as in JUY-P-153 (*N. hypsodonta*; Ercoli et al. 2021), which is also reflected in the morphology of the mure, being broad, straight, slightly oblique, and lingually positioned as on JUY-P-153. As on MUSM 4368 (Erethizontoidea gen. et sp. indet., Boivin et al. 2021), the lingual margin of the posterofossette + metafossette is positioned lingual to the mure in the mesiodistal axis.

For UFAC-CS 247, five wear stages were identified, as shown in Fig. 3. In the first and second stage (Fig. $3A_2$, A_3), the posterior arm of the paracone and the anterior arm of the mesostyle reach each other and become strongly connected, and the mesoflexus becomes a mesofossette. The posterior arm of the protocone emerges, slightly reaching the protol-

Table 2. Differences and similarities between erethizontoid species from PRE06 locality, State of Acre, Brazil.

Species	*Micronoamys candelae* Fontoura gen. et sp. nov.				*Enviramys vucetichae* Fontoura gen. et sp. nov.			*Enviramys nasifae* Fontoura gen. et sp. nov.
Specimen	UFAC-CS 247	UFAC-CS 402	UFAC-CS 255	UFAC-CS 375	UFAC-CS 253	UFAC-CS 259	UFAC-CS 252	UFAC-CS 449
Size	< *Enviramys* spp.				> *M. candelae* and < *E. nasifae*			> *M. candelae* and *E. vucetichae*
Crown high	> *Enviramys* spp.				< *M. candelae*			< *M. candelae*
Shape	oval	trapezoidal		oval (due to dental wear)	trapezoidal, more than in *M. candelae*	round to trapezoidal	round (due to dental wear)	subquadrangular
Labial margin	paracone slightly higher than mesostyle and mesio-distally aligned	paracone and mesostyle high and mesiodistally aligned		not visible due to dental wear	paracone is high and projecting labially			paracone and mesostyle mesiodistally aligned and less high than *M. candelae*
Posteroloph and hypocone area	posteroloph relatively short, disconnected from the posterior arm of hypocone (in early stages)	posteroloph relatively short, slightly connected to the posterior arm of hypocone	posteroloph connected to the posterior arm of hypocone		posteroloph connected with the posterior arm of hypocone	posteroloph subtly disconnected from the posterior arm of hypocone	posteroloph connected with the posterior arm of hypocone	posteroloph disconnected from the posterior arm of hypocone (in early stages)
Mesostyle	mesostyle and the metacone region strongly connect				posterior arm of the mesostyle slightly connected to the anterior arm of the metacone	anterior and posterior arms of the mesostyle faintly visible	posterior arm of the mesostyle appears to be present and connects to the anterior arm of the metacone	mesostyle disconnected from the metacone region
Mure	wide, almost parallel to the sagittal plane	wide and long, slightly oblique to the sagittal plane			shorter than *M. candelae* and *E. nasifae*, slightly connected to the posterior arm of the protocone			shorter than *M. candelae*, but quite robust
Hypoflexus	very oblique (in occlusal view), deep, short linguolabially and wide mesiodistally				more rounded, less deep than *M. candelae*, long linguolabially and wide mesiodistally			less rounded than *E. vucetichae*, less deep than *M. candelae*, long linguolabially
Labial flexi	subtriangular to oval shaped, paraflexus and metaflexus + posterolofleux extended more mesiodistally compared to the mesoflexus than *Enviramys*	subtriangular to oval shaped, mesoflexus mesiodistally long		oval shaped	triangular to oval shaped; linguolabially broad flexi (mainly the paraflexus and posteroflexus + metaflexus); posteroflexus + metaflexus is wider mesiodistally than other flexi; paraflexus and mesoflexus are slightly open at the labial edge		oval shaped; linguolabially broad flexi (mainly the paraflexus and posteroflexus + metaflexus); posteroflexus + metaflexus is wider mesiodistally than other flexi	oval to bean shaped; linguolabially broad flexi; mesoflexus is relatively straight and it is the smallest flexus
Second crest	one crest				two crests: labial protoloph and lingual protoloph		one crest, fused due to dental wear	one crest

oph, and the paraflexus becomes a parafossette. The posterior arm of the hypocone remains unconnected to the posteroloph. In the third stage (Fig. $3A_4$), the posterior arm of the hypocone reaches the posteroloph, resulting in the closure of the posteroflexus. In the fourth stage (Fig. $3A_5$), all the structures are strongly connected. This is followed in the fifth stage by a noticeable reduction in the size of the fossettes.

Although *Micronoamys* shares several dental similarities with *Noamys*, the available material differs markedly in smaller occlusal dimensions (about 50% smaller mesiodis-

tally and 48% smaller linguolabially) and crown height (54% smaller labially and 48% smaller lingually, compared with the M1 of *Noamys*).

Micronoamys candelae Fontoura gen. et sp. nov. differs from the two species of *Enviramys* Fontoura gen. nov. (*E. nasifae* Fontoura gen. et sp. nov. and *E. vucetichae* Fontoura gen. et sp. nov.) in size; crown high (protohypsodont) upper molars with significant unilateral hypsodonty; the mesostyle strongly connected to the posteroloph/?metacone area; a longer posterior arm of the hypocone; the mure is longer and wider as wear progresses; posteroloph relatively brief; the hypoflexus is more oblique, deeper, narrower linguolabially, and longer mesiodistally; and the labial flexi (paraflexus and metaflexus + posteroflexus) are more extended mesiodistally (Table 2). These specimens differ from *E. vucetichae* Fontoura gen. et sp. nov., UFAC-CS 449 (Fig. 2F), UFAC-CS 446 (Fig. 2H) and UFAC-CS 404 (Fig. 2G) in having a mesiodistally elongated shape; paracone and mesostyle at the same level labiolingually in occlusal view; the second crest (protoloph) formed by a single crest; the posterior arm of the protocone being shorter; posteroloph disconnected from the posterior arm of the hypocone in early stages of wear; and the metacone seemingly present. Also, they differ from *E. nasifae* Fontoura gen. et sp. nov. UFAC-CS 252 (Fig. 2K), UFAC-CS 253 (Fig. 2I) and UFAC-CS 259 (Fig. 2J) in the oval to subtriangular outline shape; having more elongated shape mesiodistally the elongation mesiodistally; higher labial cusps; long posterior arm of hypocone; posterior arm of the protocone faintly reaching both the mure and the protoloph; and in having wider posterior arm of the hypocone.

Stratigraphic and geographic range.—Type locality and horizon only.

Genus *Enviramys* Fontoura nov.

ZooBank LSID: LSID urn:lsid:zoobank.org:act:6BA1CC0B-43D0-44FC-9C8A-146280D1066F.

Type species: *Enviramys vucetichae* Fontoura gen. et sp. nov., see below.

Included species: *Enviramys vucetichae* Fontoura gen. et sp. nov. and *Enviramys nasifae* Fontoura gen. et sp. nov.

Etymology: A combination of *Envira*, in reference to the river in southwestern Brazilian Amazonia, where the fossils were discovered; and Greek *mys*, rat or mouse (Ferigolo 2025).

Diagnosis.—Small rodent displaying cheek teeth with thick enamel and non-taeniodont pattern; presence of brachydont upper molars; tetralophodont upper molars and dP4s. Upper molars with long labial crests, straight or slightly curved; and short mure. On upper molars, the mesoflexus is the last labial flexus to close with the dental wear, and the parafossette, and metafossette + posterofossette are slightly more expanded mesiodistally and labiolingually than the mesoflexus. The hypoflexus is mesiodistally long. On upper teeth, a mesiodistal enlargement of the posteroloph can be present and may correspond to a posteroloph spur or a metacone/metaloph fused with the posteroloph.

Stratigraphic and geographic range.—Solimões Formation, State of Acre, Brazil; Upper Miocene (see Fontoura et al. 2023).

Enviramys vucetichae Fontoura sp. nov.

Figs. 2F–H, 4.

ZooBank LSID: urn:lsid:zoobank.org:act:AD52267D-8BD3-4C67-9100-E5D7F4BA3662.

Etymology: In honor of María Guiomar Vucetich (Departamento Paleontología de Vertebrados, Museo de La Plata, Facultad de Ciencias Naturales y Museo, La Plata, Argentina) for her pioneering and extensive work on the taxonomy, systematics and evolutionary history of South American fossil caviomorphs.

Holotype: UFAC-CS 253, right M3 (Figs. 2F, 4).

Type locality: PRE06 locality, "Coqueiros" (08°18'12.6''S, 70°26'39.9''W), Envira River, Feijó Municipality, State of Acre, Brazil, Western Amazonia.

Type horizon: Solimões Formation, Upper Miocene (see Fontoura et al. 2023).

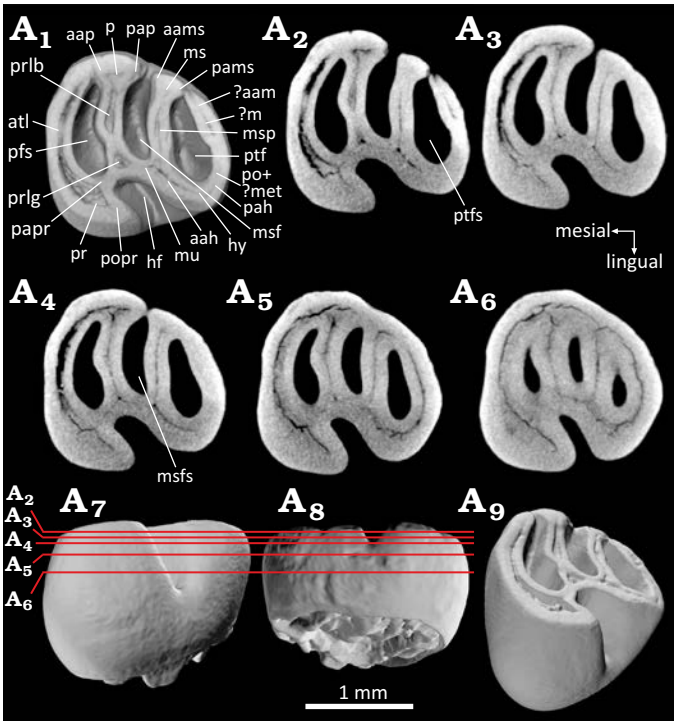


Fig. 4. Three-dimensional reconstruction of the erethizontoid rodent *Enviramys vucetichae* Fontoura gen. et sp. nov., holotype M3 (UFAC-CS 253) from PRE06 locality, State of Acre, Brazil (Upper Miocene). Tooth in occlusal (A_1), lingual (A_7), labial (A_8), and mesiolingual (A_9) views, estimate of tooth wear (A_2–A_6), the position of slices indicated in A_7, A_8. Abbreviations: aah, anterior arm of the hypocone; ?aam, anterior arm of the metacone; aams, anterior arm of the mesostyle; aap, anterior arm of the paracone; atl, anteroloph; hf, hypoflexus; hy, hypocone; ?m, metacone; ms, mesostyle; ?met, metaloph; msf, mesoflexus; msfs, mesofossette; msp, mesoloph and/or mesolophule; mu, mure; p, paracone; pah, posterior arm of hypocone; pams, posterior arm of the mesostyle; pap, posterior arm of the paracone; papr, posterior arm of the protocone; pfs, parafossette; pr, protocone; po, posteroloph; popr, posterior outgrowth of the protocone; prlb, labial protoloph; prlg, lingual protoloph; ptf, posteroflexus + metaflexus; ptfs, posterofossette + metafossette.

Diagnosis.—Small-sized upper molars with: occlusal outline wider linguolabially than longer mesiodistally; hypoflexus rounded, mesiodistally extensive, and deep; paraflexus and mesoflexus slightly open at the labial margin; oblique crests becoming progressively straighter as wear increases; protoloph composed of two crests, and the fourth transverse crest connected to the posterior arm of the hypocone; metacone and/or metaloph possibly subsumed within the posteroloph; the paracone is conspicuously robust and wide, projecting labially; well-developed posterior arm of the paracone, extending posteriorly; posterior arm of the protocone slightly connected to the lingual protoloph + mure; protocone area is similar in size to the paracone area.

Material.—Holotype and UFAC-CS 252, right M? (Fig. 2H) and UFAC-CS 259, right M3? (Fig. 2G), from the type locality and horizon.

Description.—The specimens were found at the same stratigraphic level and are considered to be a single species due to their compatible size and similar general molar morphology (Fig. 2F–H). It is a small-sized erethizontoid, especially because of its non-taeniodont pattern, its extended flexi, and the weak obliquity of lophs (Boivin et al. 2021) (similar to *Enviramys nasifae* Fontoura gen. et sp. nov.). The upper molars have a tetralophodont pattern, as in *Eopululo wigmorei* (Arnal et al. 2022), *Hypsosteiromys* (Dozo et al. 2004), *Protosteiromys pattersoni* (Pérez et al. 2018), *Steiromys detentus* (except the M3; Candela 2000), however, these taxa do not have the same general morphology, *Noamys hypsodonta* (Ercoli et al. 2021), and some unnamed erethizontid specimens from State of Acre (Campbell et al. 2006: fig. 15E). They exhibit an occlusal outline that is wider (linguolabially) than long (mesiodistally), with long flexi (mainly the paraflexus and posteroflexus + metaflexus) and curved crests that become gradually and slightly straighter as wear increases (Figs. 2F–H, 4). The HI ranges from 0.73 (UFAC-CS 259, Fig. 2G) to 0.82 (UFAC-CS 253, Fig. 2F), thus being brachydont. This variation of crown height is due to differences in the wear stage. The enamel is thick in UFAC-CS 253 and UFAC-CS 259, but in UFAC-CS 252 the enamel is damaged and eroded in several areas of the crown and occlusal surface.

UFAC-CS 252 (Fig. 2H) exhibits an advanced stage of wear and possibly marks of digestion (Kerber et al. 2017b), which obscure the observation of certain morphological features. It is tentatively identified as a molar, as the contact facets are not visible. The M3 and M3?s are distinguishable in having a distal crown region linguolabially narrower than the mesial region, a fourth transverse crest strongly curved, in addition to the absence of distal contact facet (Fig. 2F, G). Moreover, the protocone is robust and positioned more lingually than the hypocone in UFAC-CS 253 (Figs. 2F, $4A_1$) and UFAC-CS 259 (Fig. 2G). A posterior outgrowth of the protocone is projected linguodistally. The posterior arm of the protocone is oblique, directed labiodistally. On the labial margin, the paracone is the largest and highest cusp. It is more labially positioned than the mesostyle. Mesially, the anterior arm of the paracone is clearly visible, contacting the anteroloph as wear progresses (Fig. $4A_1$). Distally, the posterior arm of the paracone is highly prominent, reaching the mesostyle with advanced wear (Fig. $4A_4$). The protoloph is nearly parallel to the third crest, slightly oblique, and widened lingually. A constriction of the protoloph is visible near the mure in UFAC-CS 253 (Figs. 2F, 4). This constriction is observed in the enamel, apparently with the absence of dentine in this region. As wear progresses, the dentine begins to be exposed, as seen in UFAC-CS 259 (Fig. 2G) and UFAC-CS 253 at a more advanced stage of wear (Fig. $4A_3$). This morphology appears to represent two crests that connect to each other, one stemming from the labial side (labial protoloph) and the other from the lingual side (lingual protoloph). The lingual protoloph connects mesially but slightly to the posterior arm of the protocone, and distally to the mure. From this point, the mure is oriented distolingually, nearly perpendicular to the primary axis of the transverse lophs, thereby forming a more open angle relative to this axis (Figs. 2F–H, 4).

On the labial margin, the mesostyle is present, but smaller than the paracone. The presence of the anterior and posterior arms of the mesostyle is variable. In UFAC-CS 259 (Fig. 2G), these structures are faintly visible, whereas in UFAC-CS 253 (Figs. 2F, 4), the posterior arm of the mesostyle appears to be present and connects to the posteroloph or anterior arm of the metacone (see below). The third crest is straighter and less curved than the other crests, and may correspond to a mesoloph and/or a mesolophule. The protoloph and third crest are more obliquely oriented (labiodistally) in UFAC-CS 253 (Figs. 2F, 4) than in UFAC-CS 252 (Fig. 2H) and UFAC-CS 259 (Fig. 2G).

The presence of a metacone is considered and interpreted as the mesiodistal enlargement situated labially to/on the posteroloph (Figs. 2F, G, 4), in UFAC-CS 252 it is not possible to see due to the dental wear). Mesially, the anterior arm of the metacone is directed mesiolabially. The fourth crest is noticeably robust, possibly resulting from the fusion of posteroloph and metaloph. This crest is more curved than other crests, with its concavity facing mesially. The metaloph is not visible, as in *Noamys hypsodonta* (Ercoli et al. 2021). The hypocone has a well circular distolingual margin (except for UFAC-CS 252, Fig. 2H, in which this condition is modified by dental wear). Mesially, the anterior arm of the hypocone strongly connects to the mure and the third crest. There is no posterior outgrowth of the hypocone, as in *Nuyuyomys chinqaska* (MUSM 4324 and MUSM 4323; Boivin et al. 2021: fig 5T,X); unlike the morphology observed for example in the dP4–M1 of MACN-A 52-178 (*Parasteiromys uniformis*; Candela 1999: fig. 2; which is mentioned here solely to illustrate the condition in which this character is present, regardless of locus). UFAC-CS 252 (Fig. 2H) exhibits a distolingual elongation in the hypocone region that results from excessive wear in that area. Distally, the posterior arm of the hypocone connects to the posteroloph + ?metaloph faintly (UFAC-CS 259; Fig. 2G) or strongly (UFAC-CS 252 and 253; Fig. 2F, H). In UFAC-CS 259, the posterior arm of the hypocone is well

defined, as a constriction is present at the level of its connection with the posteroloph + ?metaloph.

The flexi are transversely expanded. The hypoflexus is broad, oblique, mesiodistally rounded, long, and deep, and never fully closes lingually under normal wear conditions. It closes only at extremely advanced stages of wear, when other flexi are no longer present. The paraflexus and mesoflexus remain slightly open in the labial margin. The first flexus to close is the paraflexus, when the anterior arm of the paracone comes into contact with the anteroloph (Fig. $4A_2$). The paraflexus and posteroflexus + metaflexus are slightly more expanded (mesiodistally and linguolabially) than the mesoflexus. The second flexus to close is the posteroflexus + metaflexus (Fig. $4A_3$), when the anterior arm of the metacone reaches the posterior arm of the mesostyle or the mesostyle itself. The last labial flexus to close is the mesoflexus (Fig. $4A_5$), when the posterior arm of the paracone joins the anterior arm of the mesostyle or the mesostyle itself. The mesoflexus is curved distally and is the narrowest flexus.

On UFAC-CS 253, five wear stages were identified, as shown in Fig. 4. In the first stage (Fig. $4A_2$), the anteroloph is strongly connected to the anterior arm of the protocone. The posterior arm of the mesostyle reaches the anterior arm of the metacone/posteroloph, a strong fusion observed in the second stage (Fig. $4A_3$). The posterior arm of the paracone remains disconnected to the anterior arm of the mesostyle, making initial contact only in the third stage of wear (Fig. $4A_4$). In the fourth stage, the flexi are strongly connected labially, and all labial fossettes are reduced in size. In the last stage (Fig. $4A_6$), the hypoflexus appears narrower, but unlike the other fossettes, which are significantly smaller, it does not become completely closed.

Enviramys vucetichae Fontoura gen. et sp. nov. differs from both *Micronoamys candelae* Fontoura gen. et sp. nov. and *Enviramys nasifae* Fontoura gen. et sp. nov. in showing occlusal outline wider linguolabially than long mesiodistally; hypoflexus rounded, mesiodistally extensive, and deep; paraflexus and mesoflexus remaining slightly open at the labial margin; oblique crests that become progressively straighter as wear increases; paracone conspicuously robust, projecting labially, with well-developed posterior arm of the paracone extending posteriorly; a dual protoloph (labial protoloph and lingual protoloph); and the fourth transverse crest connected to the posterior arm of the hypocone (Table 2). It differs from *E. nasifae* Fontoura gen. et sp. nov. (UFAC-CS 449, Fig. 2I; UFAC-CS 446, Fig. 2K; UFAC-CS 404, Fig. 2J) in smaller size, and in having a hypoflexus more rounded and wider mesiodistally in occlusal view; the posterior arm of the protocone slightly connected to the lingual protoloph + mure. *Enviramys vucetichae* Fontoura gen. et sp. nov. also differ from *Micronoamys candelae* Fontoura gen. et sp. nov. (UFAC-CS 446, Fig. 2K; UFAC-CS 402, Fig. 2B; UFAC-CS 255, Fig. 2C; UFAC-CS 247, Fig. 2A) in their larger size, labiolingually elongated and oblique crests and labial flexi, mesostyle (posterior arm of mesostyle) and metacone (anterior arm of metacone) region disconnected or slightly connected in early stages of wear; and a shallower hypoflexus, in occlusal view.

Stratigraphic and geographic range.—Type locality and horizon only.

Enviramys nasifae Fontoura gen. et sp. nov.

Fig. 2I–K.

ZooBank LSID: urn:lsid:zoobank.org:act:2C6C1A33-39EE-490A-B609-DD4877E79B52.

Etymology: In honor of Norma Nasif (Instituto Interdisciplinario de Estudios Andinos,Universidad Nacional de Tucumán, San Miguel de Tucumán, Argentina) for her significant contributions to the study of fossil caviomorphs from South America.

Holotype: UFAC-CS 449, right M1 or M2 (Fig. 2I).

Type locality: PRE06 locality, “Coqueiros” (08°18’12.6”S, 70°26’39.9”W), Envira River, Feijó Municipality, State of Acre, Brazil, Western Amazonia.

Type horizon: Solimões Formation, Upper Miocene (see Fontoura et al. 2023).

Diagnosis.—Large-sized upper molars with occlusal outline longer mesiodistally than wide linguolabially; hypoflexus oblique, long and narrow in occlusal view; paraflexus closed at the labial edge during the early stages of dental wear; mesoflexus extensive at the labial edge, closing only in advanced wear stages; transversely straight crests, with the protoloph formed by a single crest; posteroloph (+ metaloph?) faintly disconnected from the posterior arm of the hypocone in early stages of wear; presence of a mesiodistal enlargement of the posteroloph (may correspond to a posteroloph spur or a metacone/metaloph merged with the posteroloph); mesiodistal alignment of the paracone and mesostyle labially; absence of posterior arm of the paracone; posterior arm of the protocone strong and connected to the mure.

Material.—Holotype and UFAC-CS 404, right M1 or M2 (Fig. 2J) and UFAC-CS 446, left dP4 (Fig. 2K), from the type locality and horizon.

Description and comparison.—The specimens assigned to *Enviramys nasifae* Fontoura gen. et sp. nov. have compatible sizes and similar general molar morphology. They are similar in size to the early Oligocene erethizontoid *Kichkasteiromys raimondii* (M1 or M2 1.75 mm mesiodistally and 2.12 mm linguolabially; Boivin et al. 2018). The HI ranges from 0.59 (UFAC-CS 404) to 0.81 (UFAC-CS 446) (Table 1), which makes this species brachydont. The variation of crown height is due to differences in the wear.

Based on root morphology (presence of three roots: one more elongated mesiodistally in the lingual region, and two more circular in the labial region), all specimens are considered as upper teeth. The specimens have a sub-quadrangular (UFAC-CS 404, Fig. 2J and UFAC-CS 449, Fig. 2I) to oval crown outline (UFAC-CS 446, Fig. 2K). In addition, UFAC-CS 446 differs from the two other upper teeth in having a more curved anteroloph, and being comparatively longer mesiodistally, a character common in dP4s. The dis-

tal contact facets is present, whereas the mesial facet cannot be assessed due to lateral enamel wear. Hence, we interpret UFAC-CS 446 as dP4 and UFAC-CS 404 (Fig. 2J) and UFAC-CS 449 (Fig. 2I) as M1 or M2, as they exhibit both anterior and posterior contact facets. The three specimens have an occlusal outline longer than it is wide, as in *Noamys hypsodonta* (Ercoli et al. 2021), *Parasteiromys* (Candela 1999) and *Micronoamys candelae* Fontoura gen. et sp. nov. The crests are transversely straight. Upper molars and dP4 display a tetralophodont pattern (see description and comparisons in *E. vucetichae* Fontoura gen. et sp. nov.). The cusps on the labial margin are well marked on UFAC-CS 449 (Fig. 2I); however, it is not possible to determine precisely their size due to dental wear. The paracone appears, however, as the largest cusp, and is aligned with the mesostyle on a mesiodistal axis.

Mesially, the anteroloph is slightly curved on UFAC-CS 404 (Fig. 2J), and straighter on UFAC-CS 449 (Fig. 2I). Along the labial margin, it is connected to the anterior arm of the paracone, seemingly right after tooth eruption. The posterior arm of the paracone is absent. The protocone is noticeably robust, elongated mesiodistally and linguolabially on UFAC-CS 449 (Fig. 2I), probably due to greater wear in this area, specifically in this specimen. Distally, the protoloph is straight, formed by a single crest, and connects to the posterior arm of the protocone mesiolingually; it strongly connects to the mure distolingually.

The third transverse crest, likely a mesoloph, is either straight (UFAC-CS 449, Fig. 2I) or slightly oblique distolabially (UFAC-CS 404, Fig. 2J and UFAC-CS 446, Fig. 2K), possibly due to wear progress. Both the protoloph and third crest exhibit a slight mesiodistal widening at the midpoint of the crests. On their lingual margin of them, the mure is strongly connected to the third transverse crest distally, and to the protoloph, mesially. On the labial margin, it joins a mesostyle projecting toward the posteroloph (or the anterior arm of the metacone; see below) as on UFAC-CS 449 (Fig. 2I), eventually reaching it as dental wear progresses (UFAC-CS 404, Fig. 2J and UFAC-CS 446, Fig. 2K). On UFAC-CS 404 (Fig. 2J), a short anterior arm of the mesostyle can be observed, directed toward the paracone. The paracone and mesostyle (or anterior arm of the mesostyle) remain unconnected, and only become so at an advanced stage of wear.

The last crest, the posteroloph, is more oblique and may (UFAC-CS 446, Fig. 2K and UFAC-CS 404, Fig. 2J) or may not (UFAC-CS 449; Fig. 2I) fully connect to the hypocone on the linguodistal margin. This character depends on the stage of wear. The posteroloph is wider mesiodistally than the other lophs. The specimen UFAC-CS 404 (Fig. 2J) exhibits a mesially oriented projection, possibly corresponding to a posteroloph spur. UFAC-CS 446 (Fig. 2K) exhibits a broader posteroloph, potentially representing a fusion of the posteroloph and the posteroloph spur and/or metacone/metaloph. In UFAC-CS 449 (Fig. 2I), these structures seem to be absent or indistinct (as in *Noamys hypsodonta*; Ercoli et al. 2021), and the posteroloph is not as wide. The metacone seems to be absent (indistinct), but this cusp can be subsumed within the posteroloph (i.e., present but indistinct). However, as all specimens exhibit dental wear, it is not possible to assess the presence of this structure. This morphological variation of the posteroloph may represent different dental loci, a pattern observed in other caviomorphs such as *Sallamys pascuali* (upper molar; Lavocat 1976), *Noamys hypsodonta* (DP4-M1; Ercoli et al. 2021), *Hypsosteiromys* (P4, Candela 1999; M1, Dozo et al. 2004), *Eosteiromys homogenidens* (P4, Candela 2003) and *Parasteiromys* (upper tooth, Candela 1999), or reflect different stages of dental wear, either highlighting or obscuring certain structures. However, as these specimens are isolated teeth and not in connection, it is not possible to go any further in terms of identification.

The hypocone lies on the distolingual margin. It shows a tendency to connect (via a short posterior arm of the hypocone) to the fourth transverse crest on UFAC-CS 449 (Fig. 2I). The anterior arm of the hypocone connects strongly to the mure and the third crest. The intersection of these three crests forms a robust structure. The anterior arm of the hypocone is oriented more labiomesially compared with this structure in *Micronoamys candelae* Fontoura gen. et sp. nov. The distolingual aspect of the hypocone is noticeably curved, with no posterior/anterior outgrowth (unlike MACN-A 52-178, *Parasteiromys uniformis*; Candela 1999: fig. 2).

The flexi are oval to bean shaped. The mesoflexus is relatively straight and it is the smallest flexus, followed by the paraflexus. The metaflexus + posteroflexus is the most mesiodistally extended flexus, and it is broader in the lingual region. The hypoflexus is oblique, long and narrow in the occlusal view. The first flexus to close is the paraflexus, in early stages of wear, followed by the metaflexus + posteroflexus, and finally the mesoflexus, which closes only in advanced stages of wear.

Enviramys nasifae Fontoura gen. et sp. nov. differs from *Micronoamys candelae* Fontoura gen. et sp. nov. and *Enviramys vucetichae* Fontoura gen. et sp. nov. in a larger size (approximately 15% and 2% larger, respectively, based on size comparisons using mean occlusal area [mdl × mw]); hypoflexus narrow in occlusal view; absence of posterior arm of the paracone; and strong posterior arm of the protocone connected to the mure (Table 2). The material differs from *Micronoamys candelae* Fontoura gen. et sp. nov. in having: upper molars more elongated linguolabially; a short mure; a mesostyle disconnected of the posteroloph/metacone region, when there is no dental wear; a smaller size difference between the paraflexus and metaflexus + posteroflexus vs. mesoflexus; and a hypoflexus less oblique, shallower and longer in occlusal view. Also, it differs from UFAC-CS 253 (Fig. 2F), UFAC-CS 259 (Fig. 2G) and UFAC-CS 252 (Fig. 2H) (*E. vucetichae* Fontoura gen. et sp. nov.) in exhibiting a proportionally more quadrangular crown outline in the upper molars, whereas specimens of *E. vucetichae* Fontoura gen. et sp. nov. display crowns that are relatively longer labiolingually than mesiodistally; paraflexus closed at the labial

margin during the early stages of wear; mesoflexus wide at the labial margin; and hypoflexus shorter mesiodistally than *E. vucetichae* Fontoura gen. et sp. nov.

Stratigraphic and geographic range.—Type locality and horizon only.

Octochinchilloi Boivin in Boivin, Marivaux, and Antoine, 2019

Chinchilloidea Bennett, 1833

Genus *Microscleromys* Boivin & Walton in Boivin et al., 2021

Type species: *Microscleromys paradoxalis* Boivin & Walton in Boivin et al., 2021; CVP 13B locality, Fish Bed near Casa Cuzco, La Venta Badlands, upper Magdalena Valley, Huila Department, Colombia; late Middle Miocene.

cf. *Microscleromys* sp.

Figs. 2E, 5.

Material.—UFAC-CS 190, right m1 or m2 from PRE06 locality, "Coqueiros" (08°18'12.6"S, 70°26'39.9"W), Envira River, Feijó Municipality, State of Acre, Brazil, Western Amazonia; Upper Miocene (see Fontoura et al. 2023).

Description.—The only lower molar discovered displays a trilophodont pattern (Fig. 2E), unlike, e.g., *Drytomomys* (Kerber et al. 2017c), *Protadelphomys* (= *Gaimanomys*; Vucetich and Bond 1984) and *Incamys* (Busker and Dozo 2017). The occlusal crown outline is rectangular, being longer (mesiodistally) than it is wide (labiolingually). The maximum mesiodistal length is 2.26 and the maximum width is 1.98 mm (Table 1), larger than the late Oligocene *Chambiramys* (Contamana, Peru; m1–m2 with mean length of 1.86 mm mesiodistally and 1.59 mm linguolabially; Boivin et al. 2017a), *Microscleromys paradoxalis* (from Tarapoto, Peru; m1(?)–m2(?) with mean length of 1.86 mm mesiodistally and 1.62 mm linguolabially; Boivin et al. 2021) and *Microscleromys cribriphilus* (from Tarapoto, Peru; m1–m2 with mean length of 1.57 mm mesiodistally and 1.35 mm linguolabially; Boivin et al. 2021) and smaller than other chinchilloids, such as *Scleromys* (Fields 1957; Kramarz 2006), *Saremmys* (Busker et al. 2019), *Prolagostomus* (Ameghino 1887), *Potamarchus*, *Phoberomys*, *Neoepiblema* (Kerber et al. 2017c), *Miochinchilla* (Croft et al. 2021), *Protadelphomys* (= *Gaimanomys*; Vucetich and Bond 1984) and *Garridomys* (Kramarz et al. 2013). The maximum crown height is 1.30 mm (labially) and 1.01 mm (lingually), higher than other m1/m2 specimens of *Microscleromys* sp. from Tarapoto (TAR-31, Peru; Boivin et al. 2021: fig. 9), except for MUSM 4647 (left m1 or m2; Boivin et al. 2021: fig. 9H). Nevertheless, the HI of 0.58 is close to the expected value for the m1 and m2 of this group (MUSM 4647, 4650–4643; see Boivin et al. 2021). The original HI was likely somewhat larger prior to wear, but it would have remained within the range of brachyodonty, differingt from that in e.g., species of *Saremmys*, *Miochinchilla*, *Garridomys*, *Incamys*, *Scleromys*, *Neoepiblema*, and *Phoberomys*. The cristids are thinner and less oblique than in species of *Saremmys* but similar to that in species of e.g., *Chambiramys*, *Incamys*, and *Scleromys*. In addition, the cristids are not developed as laminae (as seen in species of *Neoepiblema*, *Phoberomys*, and *Miochinchilla*).

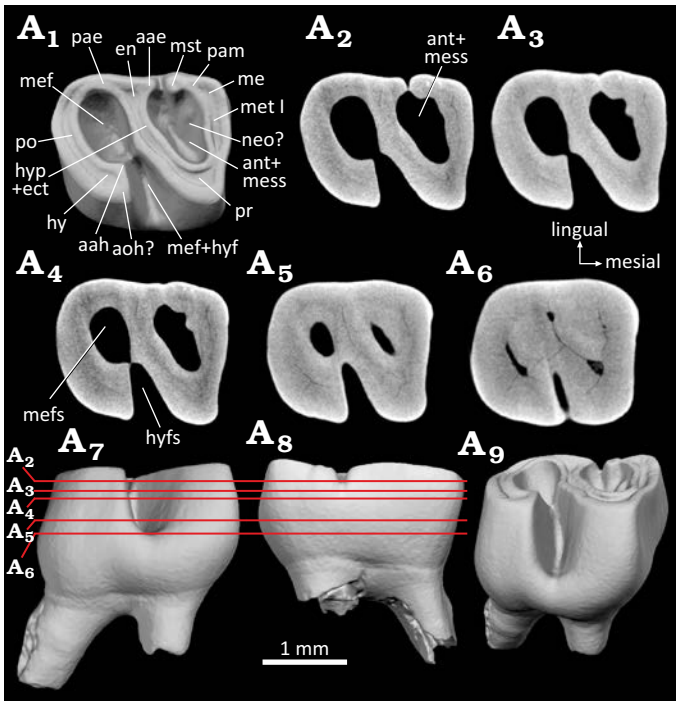


Fig. 5. Three-dimensional reconstruction of the chinchilloidean rodent cf. *Microscleromys* sp. m1 or m2 (UFAC-CS 190) from PRE06 locality, State of Acre, Brazil (Upper Miocene). Tooth in occlusal (A_1), labial (A_7), lingual (A_8), and mesiolabial (A_9) views, estimate of tooth wear (A_2–A_6), the position of slices indicated in A_7, A_8. Abbreviations: aae, anterior arm of the entoconid; aah, anterior arm of the hypoconid; ant, anteroflexid; ants, anterofossettid; aoh, anterior outgrowth of the hypoconid; ect, ectolophid; en, entoconid; hy, hypoconid; hyf, hypoflexid; hyfs, hypofossettid; hyp, hypolophid; me, metaconid; mef, metaflexid; mefs, metafossettid; met i, metalophulid i; mes, mesoflexid; mess, mesofossettid; mst, mesostylid; neo?, neomesolophid; pae, posterior arm of the entoconid; pam, posterior arm of the metaconid; po, posterolophid; pr, protoconid.

The mesialmost portion of the tooth reveals the presence of the metalophulid I, a linear straight structure that exhibits a constriction in the labial region, where it joins with the protoconid (Figs. 2E, 5). In the lingual region, the metalophulid I connects to the metaconid. The metaconid bears a posterior arm, which projects distally along the lingual margin, ultimately reaching the mesostylid, as seen in species of *Chambiramys*. The mesostylid is small, but clearly visible and rounded without either anterior and posterior arms, although it already exhibits superficial wear (Figs. 2E, $5A_1$). On the labial margin, the protoconid is prominent, extending distolingually to integrate with the ectolophid, from which it is almost indistinguishable. The hypolophid is slightly oblique distolingually and tends to form a continuous cristid with the protoconid + ectolophid, as in species of e.g., *Garridomys* and most dinomyids. Along with the lingual margin, the entoconid is distinctly identifiable. Mesially, the anterior arm of the entoconid is present

but remains disconnected from the mesostylid in early wear stages (Fig. 5A$_2$). This connection appears progressively with advancing dental wear (Fig. 5A$_2$–A$_4$). Distally, the posterior arm of the entoconid is strongly connected to the posterolophid, unlike in *Chambiramys* and *Garridomys*.

The posterolophid is robust and curved. It joins the large hypoconid at the level of its labial margin. On the anterolabial margin of the hypoconid, the enamel layer seems to exhibit a very tiny pinch, that might represent a rudimentary anterior outgrowth (see Fig. 5A$_2$–A$_6$). Between the hypoconid and the ectolophid + hypolophid, in the mesiolingually direction, a lower connection of both structures is established via the anterior arm of the hypoconid. This junction is only formed in advanced stages of wear (see Fig. 5A$_5$); until then, the hypoconid and ectolophid + hypolophid remain isolated. Thus, we recognize this configuration as a pseudotaeniodont pattern (see Boivin et al. 2021), as in species of e.g., *Chambiramys*. A very subtle structure is observed in the anteroflexid + mesoflexid, in the labiodistal margin of the metaconid and the metalophulid I, emerging exclusively in advanced stages of wear (see Fig. 5A$_3$). This feature may represent a rudimentary neomesolophid. However, additional specimens are required to elucidate this morphology.

The anteroflexid + mesoflexid exhibit a broad, oval-triangular configuration, with no discernible separation between them, at any stages of wear. The lingual margin is longer than the labial one. The metafossettid and hypoflexid remain initially conjoined, with the metafossettid presenting an oval morphology, whereas the hypoflexid is characterized by a more linear conformation, distolingually oriented. As dental wear progresses, the metafossettid and hypoflexid become distinctly separated (Fig. 5A$_4$, A$_5$; as seen in species of e.g., *Garridomys*, and unlike in these of e.g., *Saremmys*, *Drytomomys*), with the metafossettid adopting a morphology similar to that of the anteroflexid + mesoflexid.

UFAC-CS 190, five stages of wear were identified, as shown in Fig. 5. In the first stage (Fig. 5A$_2$), the anterior arm of the entoconid is observed reaching the mesostylid, the anteroflexid + mesoflexid becoming anterofossettid + mesofossettid. In the second stage (Fig. 5A$_3$), the connection between the anterior arm of the entoconid and the mesostylid is well established. Between the mesostylid and the metalophulid I, a possible neomesolophid begins to emerge as a "spur", oriented distolabially. In the third stage (Fig. 5A$_4$), it is observed that the spur (possible neomesolophid) does not extend distally. The anterior arm of the hypoconid reaches the ectolophid + hypolophid, thereby separating the hypoflexid from the metaflexid (as such becoming the metafossettid). The areas of the hypoconid and protoconid become increasingly robust. In the fourth stage (Fig. 5A$_5$), the connection between the anterior arm of the hypoconid and the ectolophid is well established. The area of the metafossettid, which maintains an oval shape, and the combined area of the antefossettid and mesofossettid, which have an oblique and elongated shape oriented distolingually and mesiolabially, are significantly reduced. The hypoflexid closure occurs in the fifth stage (Fig. 5A$_6$), while all other fossettids and associated structures are no longer visible.

It is worth mentioning that this specimen is the only one from this locality that presents this combination of morphological features. Although the overall occlusal morphology is similar to that of UFAC-CS 205 (see below), it is significantly smaller in total size, including crown height. It shows a morphology more similar to species of *Microscleromys* than to lower molars of any other species collected from this locality so far.

Genus "*Scleromys*" Ameghino, 1887

Type species: *Scleromys angustus* Ameghino, 1887; Pinturas and Santa Cruz formations, Santa Cruz province, Argentina; late Early Miocene

Figs. 2L, 6.

Material.—UFAC-CS 205, right m1 or m2? from PRE06 locality, "Coqueiros" (08°18'12.6''S, 70°26'39.9''W), Envira River, Feijó Municipality, State of Acre, Brazil, Western Amazonia; Late Miocene (see Fontoura et al. 2023).

Description.—As in Boivin et al. (2021), because the northern forms referred to as "*Scleromys*" (Walton 1997; Boivin et al. 2017a) still require revision, we keep the material from TAR-31 in open nomenclature as "*Scleromys*" sp. This molar is high-crowned, with a maximum crown height of

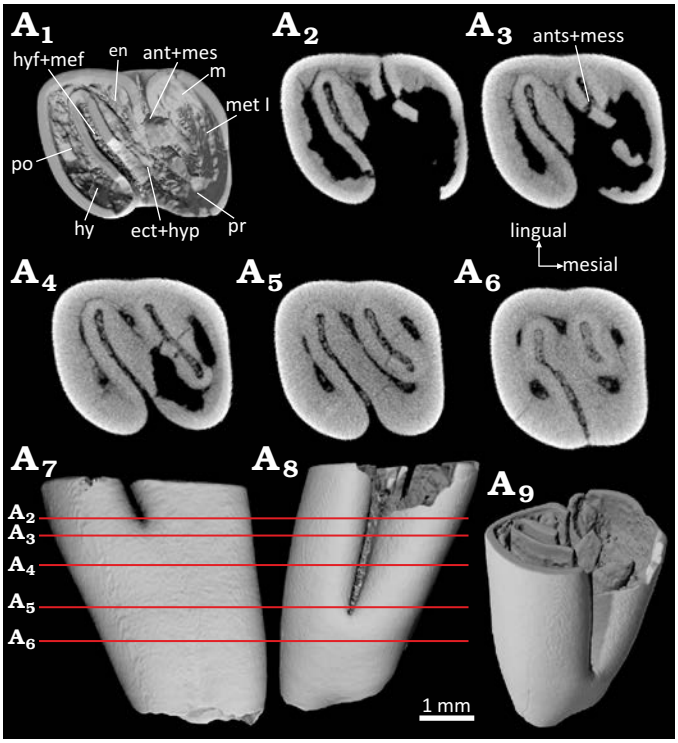


Fig. 6. Three-dimensional reconstruction of the chinchilloidean rodent "*Scleromys*" sp. m1 or m2? (UFAC-CS 205) from PRE06 locality, State of Acre, Brazil (Upper Miocene). Tooth in occlusal (A$_1$), labial (A$_7$), lingual (A$_8$), and distolabial (A$_9$) views, estimate of tooth wear (A$_2$–A$_6$), the position of slices indicated in A$_7$, A$_8$. Abbreviations: ant, anteroflexid; ants, anterofossettid; en, entoconid; ect, ectolophid; hy, hypoconid; hyf, hypoflexid; hyp, hypolophid; m, metaconid; mef, metaflexid; met i, metalophulid i; mes, mesoflexid; mess, mesofossettid; pr, protoconid; po, posterolophid.

~4.54 mm and a HI of 1.38. The specimen seemingly retained roots, which were possibly lost during fossilization. Thus, it would be protohypsodont as species of *Garridomys* and *Scleromys*/"*Scleromys*" (Fields 1957; Walton 1997; Kramarz 2006; Kramarz et al. 2013). This tooth is the largest specimen analyzed in this study. The maximum mesiodistal length is 3.30 mm and the maximum width is 2.94 mm (Table 1). It is much smaller than *Olenopsis* (Walton 1997), *Eusigmomys oppositus* (Vucetich 1984); *Eusigmomys* cf. *E. oppositus* (Kramarz et al. 2025) and *Scleromys* spp. (e.g., m1 with a mean length of 4.84 mm and m2 with 4.99 mm in *S. quadrangulatus*; lower molar with 6.46 mm in *S. angustus*; m1 with 4.73 mm, and m2 with 5.06 mm in *S. osbornianus*; Kramarz 2006), smaller than "*Scleromys*" *schurmanni*, "*S.*" *colombianus*, and "*Scleromys*" sp. from TAR-31 (Peru), and slightly larger than *Microscleromys* sp. (Walton 1997; Boivin et al. 2021). Although fractured in the mesialmost flexid region, computed microtomography enabled an assessment of wear estimation and the observation of structures that were not visible in occlusal view (Fig. 5). It has a trilophodont pattern (e.g., as in *Garridomys*, *Eusigmomys oppositus*, and unlike *Neoreomys* and *Maquiamys praecursor*), is taeniodont, exhibits a rhomboidal or rectangular occlusal shape, as in *S. quadrangulatus* and *S. angustus*, and has oblique and parallel cristids, unlike *Maquiamys praecursor.* Unlike *S. quadrangulatus*, it is much longer mesiodistally than wide (in early stages of wear). As in species of *Scleromys*, it has the typical S-shaped pattern (Kramarz 2006), also resembling these of *Garridomys* and *Eoviscaccia* in juvenile stages (Kramarz et al. 2013). The thickness of the enamel layer is homogenous between the leading and trailing edges of the lophids. The lingual margin is quite straight and long, while the labial margin is more curved and shorter.

The metalophulid I, located in the mesialmost region, is robust and slightly curved. It connects to the protoconid on the labial side of the tooth and to the metaconid on the lingual side. Despite wear, it is possible to visualize the regions where these two cuspids would normally occur, as they are wide (Fig. $6A_1$). These cuspid regions are well rounded. The neomesolophid appears to be absent in the current wear stage, as well as in more advanced stages of wear (see Fig. 6). If present in the unworn tooth, it, would probably be fused with the metalophulid I in early wear, as well as the anterofossettid, similarly to *Scleromys angustus* and *S. osbornianus*, which have trilophodont molars during most of the animal's lifetime (Walton 1997). In comparison, *Scleromys quadrangulatus*, "*Scleromys*" *schurmanni*, and "*Scleromys*" *colombianus* have lower molars with more persistent neomesolophid and anterofossettid (Walton 1997; Kramarz 2006). The middle ridge is composed of the protoconid + ectolophid + hypolophid + entoconid, forming a linear, robust, oblique cristid, directed distolingually, and, as such, resembling the diagonal structure observed in lower molars of species of *Garridomys* and the Patagonian *Scleromys*. Distally, the posterolophid connects labially to the hypoconid, and extends lingually to reach the entoconid, unlike in species of *Garridomys* in early wear. The posterolophid is a robust and curved cristid. The hypoconid is located slightly lingual to the protoconid, on the mesiodistal axis. Its margin is well rounded, as in *Maquiamys praecursor* and *S. angustus*.

The mesoflexid is linear and oblique. As wear progresses, the lingual border of this flexid closes quickly, resulting in the formation of a fossettid (Fig. $6A_3$), as in *S. osbornianus* and unlike in *S. quadrangulatus*. It becomes significantly smaller linguolabially as wear progresses (Fig. 6).

The most distal flexid is the confluence between the hypoflexid from the labial region, and the metaflexid from the lingual region. It is wider than the mesial flexid, but also linear and oblique. These flexids only separate when dental wear is very advanced (Fig. $6A_6$), as seen in species of *Garridomys*. Hence, we recognize this specimen as taeniodont in early stages of wear. The hypostriid is high, but not as high as in *Saremmys ligcura* (Busker et al. 2019).

On UFAC-CS 205, five stages of wear were identified, as shown in Fig. 6. Due to a fracture on the surface, the early stages (Fig. $6A_2$, A_3) could not be fully assessed. However, in the first stage (Fig. $6A_2$), the initial closure of the mesial flexid (probably anteroflexid + mesoflexid) can be observed on the lingual margin. In the second stage (Fig. $6A_3$), the anterofossettid + mesofossettid are fully closed, and the contact on the lingual margin appears to be strongly fused. In the third and fourth stage, the flexids are reduced in their linguolabial extension, especially the mesial flexid. In the fifth stage (Fig. $6A_6$), the hypoflexid becomes labially closed. There is a tendency for the separation of the hypoflexid from the metaflexid, indicated by the projection of the posterior arm of the hypoconid and the curvature of the ectolophid, although no connection is formed (confirming the taeniodont pattern). The mesial fossettid occupies less than half of the linguolabial extension.

Noteworthy, this tooth is the one and only specimen from the material of the PRE06 fossil-bearing locality that displays this morphology. It shows a morphology more similar to *Scleromys*/"*Scleromys*" than to any other taxon reviewed and to the other lower molars collected at the same locality. In its stage of wear, the absence of anterofossettid in UFAC-CS 205 suggests that it could be more related to *S. angustus* and *S. osbornianus*. However, this tooth from PRE06 locality is clearly smaller than these species and the other species attributed to *Scleromys*/"*Scleromys*". According to Kramarz (2006), size is an important criterion for distinguishing species within this genus, thus UFAC-CS 205 could document a new taxon. Due to the fact that it is a single isolated and fragmented tooth, we cautiously keep it with an open nomenclature pending more informative data.

Discussion

Dental morphology and taxonomic remarks.—In this study, we described new dental remains of caviomorph rodents from Upper Miocene Solimões Formation, exposed

along the Envira River in Brazil (State of Acre, Western Amazonia). The fossils documented here comprise three new species of Erethizontoidea, as well as new records of cf. *Microscleromys* sp. and cf. "*Scleromys*" sp. Extinct porcupines were traditionally referred to Erethizontidae, excluding the recognition of possible stem-erethizontoids until recently (see Boivin et al. 2018, 2021). An extend phylogenetic analysis would be necessary to determine the position of several erethizontoids with more certitude (i.e., *Kichkasteiromys*, *Eopululo*, *Cholamys*, *Parasteiromys*, *Microsteiromys*, *Nuyuyomys*, and *Noamys*) and test the absence of stem-erethizontoids. Hence, we assign these specimens to Erethizontoidea rather than Erethizontidae as a conservative taxonomic decision.

Micronoamys candelae Fontoura gen. et sp. nov. is distinguished by a unique combination of morphological features (as the *Micronoamys* Fontoura gen. nov.). This taxon shows morphological similarity with *Noamys hypsodonta* (e.g., tetralophodont pattern; unilateral hypsodonty; indistinct metaloph; labial flexi exhibiting a triangular or oval shape, mesiodistally expanded; hypoflexus very oblique and short), and a thicker enamel layer than *Noamys*.

Enviramys Fontoura gen. nov. is based on the combination of several features, such as: (i) small size; (ii) a tetralophodont pattern of upper molars and dP4s; (iii) brachydont molars; (iv) long hypoflexus; (v) long crests, straight or slightly oblique; (vi) the mesoflexus being the last labial flexus to close with dental wear and the parafossette, mesoflexus and metafossette + posterofossette displaying comparable amplitudes (mesiodistally and labiolingually); (vii) elongated crests, straight or slightly oblique; (viii) a fourth transverse crest (posteroloph) variably connected to the posterior arm of the hypocone; (ix) short mure; (x) a mesiodistal enlargement of the posteroloph that may correspond to a posteroloph spur or a metacone/metaloph merged with the posteroloph.

Enviramys Fontoura gen. nov. comprises two species that differ in a suite of characters not attributable to differences in dental loci. Although the material referred to *E. vucetichae* Fontoura gen. et sp. nov. consists exclusively of M3s and *E. nasifae* Fontoura gen. et sp. nov. is represented by non-M3 upper molars, the differences between them exceed the range of variation usually observed among dental loci in erethizontids with complete upper toothrows (e.g., species of *Coendou*, *Hypsosteiromys*, *Neosteiromys*, and extant erethizontids; Candela 1999, 2003). In these taxa, M3s are typically smaller, more trapezoidal, and tend to show reduced or absent metalophs, and more curved lophs compared to anterior molars. Several of the features observed here are inconsistent with this pattern alone, e.g., a rounded and mesiodistally expansive hypoflexus (*E. vucetichae* Fontoura gen. et sp. nov.) as opposed to a narrow one in occlusal view (*E. nasifae* Fontoura gen. et sp. nov.); a paraflexus that remains slightly open at the labial margin (*E. vucetichae* Fontoura gen. et sp. nov.) rather than closing prematurely during dental wear (*E. nasifae*); and a protoloph composed of two crests (*E. vucetichae* Fontoura gen. et sp. nov.) instead of a single crest (*E. nasifae* Fontoura gen. et sp. nov.).

Enviramys vucetichae Fontoura gen. et sp. nov. is characterized by: (i) occlusal outline wider than long; (ii) hypoflexus rounded and mesiodistally extensive; (iii) oblique crests that become progressively straighter as wear increases; (iv) paraflexus slightly open at the labial edge; (v) a second transverse crest composed of two crests; and (vi) posterior arm of the protocone slightly connected to the lingual protoloph + mure.

In contrast, *Enviramys nasifae* Fontoura gen. et sp. nov. differs in: (i) its larger size (approximately 15% larger than *Micronoamys candelae* Fontoura gen. et sp. nov. and 2% than *E. vucetichae* Fontoura gen. et sp. nov.); (ii) a quadrangular occlusal outline; (iii) straight crests; (iv) narrow hypoflexus in occlusal view; (v) absence of posterior arm of the paracone; (vi) posterior arm of the protocone strongly connected to the mure; (vii) the protoloph formed by a single crest; (viii) paraflexus closed at the labial margin during the early stages of wear; and (ix) mesoflexus wide at the labial margin, closing only in advanced wear. The combination of size, crown proportions, crest organization, and occlusal geometry supports the recognition of two distinct species rather than locus variation of a single taxon. Nevertheless, although the number of specimens available for each new species is limited, we consider it sufficient. An extensive systematic comparison of dental associations was carried out (see Material and methods) on all specimens collected from the locality in question (Envira River, State of Acre). Furthermore, comparisons between different wear stages were conducted based on virtual wear methodology, and no other specimen from the same assemblage appears to group taxonomically with these materials in terms of morphology and/or size.

One of the two chinchilloid isolated specimens is assigned to cf. *Microscleromys* sp. based on the combination of several features, such as: (i) molar brachydonty; (ii) pseudo-taeniodont pattern; (iii) metalophulid I with a constriction in the labial region (= groove on the metalophulid I; Boivin et al. 2021); and (iv) mesostylid without anterior and posterior arms (Walton 1997; Boivin et al. 2021). As it is based on a single isolated tooth, its species-level attribution is not reliable, despite the reasonable preservation state of the specimen. Due to its diminutive size, it may be closer to *Microscleromys cribriphilus*, the smallest known species of the genus (Walton 1997).

Finally, the remaining tooth is assigned to "*Scleromys*" sp., based on the presence of: (i) trilophodont pattern; (ii) S-shaped crest pattern; (iii) taeniodont pattern; iv) presence of a homogenous enamel layer; (v) protohypsodont molars; (vi) deep hypostriid; (vii) oblique cristids; (viii) narrow, labiolingually elongated and oblique flexids (more than cristids); and (ix) absence of neomesolophid (Kramarz 2006). Given the small size of this specimen and considering that teeth size is regarded as an important diagnostic character for the identification of the species of *Scleromys* (Kramarz 2006), this record may represent a new taxon

within the group. However, as it consists of a single isolated and fragmentary tooth with a somewhat conservative morphology, we keep this taxon in open nomenclature, pending additional dental remains.

Comparisons.—The new taxa identified as erethizontoids exhibit strong affinities with other members of this superfamily, compared to other caviomorph superfamilies. This is particularly substantiated by their non-taeniodonty, extended flexi, and weak obliquity of lophs (Boivin et al. 2021). The new erethizontoids differ from other taxa of this group, such as: e.g., species of *Nuyuyomys* (Boivin et al. 2021), *Noamys* (Ercoli et al. 2021), *Microsteiromys* (which is known only through lower molars; Boivin et al. 2021), *Shapajamys* (Boivin et al. 2018), *Palaeosteiromys* (Boivin et al. 2017a), *Eopululo* (Frailey and Campbell 2004), *Protosteiromys* (Wood and Patterson 1959), *Branisamyopsis* (Candela 2003), *Hypsosteiromys* (Dozo et al. 2004), *Parasteiromys* (Candela 1999), *Eosteiromys*, *Steiromys*, and *Neosteiromys* (Candela 2004) in having a smaller size; e.g., *Branisamyopsis* (Kramarz 2004), *Parasteiromys*, *Neosteiromys*, *Nuyuyomys*, *Eosteiromys annectens* (Kramarz 2004) and *Palaeosteiromys* in having tetralophodont upper molars. This character is not common in medium and large-sized erethizontoids but is seen mostly in small erethizontoids (e.g., *Noamys*; Ercoli et al. 2021).

In addition, they differ from *Eosteiromys annectens* in having non-taeniodont upper teeth; from species of *Parasteiromys* in developing a mure; from these of *Hypsosteiromys*, *Parasteiromys*, and *Neosteiromys* in displaying a metaloph indistinct or absent; from cf. *Microsteiromys* sp. (Candela et al. 2021: fig. 3a–a') in having subequal length and width, or a width exceeding the length; and from species of *Branisamyopsis* and *Neosteiromys*, in having a paraflexus disconnected from the hypoflexus (i.e., non-taeniodont pattern).

Micronoamys Fontoura gen. et sp. nov. differs from all other taxa of this group (except from *Noamys*), in having a unilateral hypsodonty and indistinguishable metacone. In addition to the aforementioned characters, *Enviramys* Fontoura gen. nov. differs from *Noamys* in having brachydont teeth; flexi longer linguolabially; long crests, straight or slightly oblique; quadrangular to rounded outline shape; and hypoflexus neither as oblique, deep nor as short in occlusal view as observed in *Noamys*.

Nevertheless, *Enviramys* Fontoura gen. nov. shares similarities in form and size with the Late Miocene erethizontoid from the State of Acre and Juruá rivers, Peru (Campbell et al. 2006: fig. 15A), and with the Late Miocene Erethizontidae cf. *Microsteiromys* sp. from Palo Pintado, Argentina (Candela et al. 2021: fig. 3a–a') in: (i) small size; (ii) tetralophodont pattern; (iii) labiolingually elongated crests and flexi; (iv) short mure; (v) wide hypoflexus extending linguolabially (only for the erethizontoid from the Acre River); and (vi) a constriction labiodistally to the hypocone between its posterior arm and the posteroloph.



Fig. 7. Paleoenvironment and life reconstructions of *Enviramys vucetichae* Fontoura gen. et sp. nov. (bellow), *E. nasifae* Fontoura gen. et sp. nov. (upper right) and *Micronoamys candelae* Fontoura gen. et sp. nov. (upper left). Art by Caetano Soares (Universidade Federal de Pelotas, Brazil).

Paleoenvironmental implications.—Based on morphological comparisons with modern taxa and their distribution in ecosystems, the presence of erethizontoids can be viewed as a paleoenvironmental indicator of forested habitats, given arboreality and strong association with tropical forest environments (Ercoli et al. 2021; Fig. 7).

The potential coexistence of some chinchilloids (*Neoepiblema* and Dinomyidae), the caviid *Cardiatherium* (Fontoura et al. 2023), and the erethizontoids reported here suggests a warm and humid climate and mixed vegetation cover, with both open and forested areas in this region of the Amazonia during the time of deposition of these strata (Walton 1990; Kerber et al. 2017c; Stutz et al. 2023). The occurrence of *Neoepiblema* and *Cardiatherium* is not by itself diagnostic of humid environments; however, when considered within the broader geological and paleontological framework, their presence is consistent with previously proposed wetland-dominated systems. A similar interpretation is inferred for La Venta, Fitzcarrald Arch, and TAR-31 assemblages, with humid forested areas associated to grasslands or scrubs in a humic environment (Walton 1990; Tejada-Lara et al. 2015; Marivaux et al. 2020; Stutz et al. 2022, 2023; Carrillo et al. 2023).

Fauna comparisons and biogeochronologic implications.—The material described here contributes to further understanding of the biogeographic patterns of the northern

caviomorphs in South America during the Neogene. Small Miocene erethizontoids are very rare, and so far known only from State of Acre in Brazil, La Venta in Colombia (Walton 1997), MD-67 (Upper Madre de Dios; Antoine et al. 2013) and TAR-31 in Peru (Boivin et al. 2021). *Microscleromys* is known only from Middle Miocene of Colombia and Peru. The new record reported here represents for now the most recent and easternmost occurrence of this genus. *Scleromys*/"*Scleromys*" has widespread geographic (Argentina, Ameghino 1887, 1894; Kramarz 2006; Cerdeño and Vucetich 2007; Brazil, Kerber et al. 2017c; Chile, Flynn et al. 2008; Peru, Antoine et al. 2013, 2016; Tejada-Lara et al. 2015; Boivin et al. 2021; and Colombia, Fields 1957; Walton 1997; Boivin et al. 2021) and temporal distributions (since the Early Miocene; see Boivin et al. 2021), and its occurrence at the PRE06 locality could then have been expected. As for the genus *Acarechimys* (see Arnal et al. 2017; Fontoura et al. 2024), which occurs from the Lower Miocene to the Upper Miocene, ranging from southern Argentina to Brazilian Amazonia, such widespread geographic and stratigraphic distributions may be overestimated. It is unlikely for a single genus to persist over such an extended period (Jablonski 2008). It is possible that these records represent distinct taxa exhibiting evolutionary convergences or very conservative dental evolution. As pointed out by Boivin et al. (2017a, 2021), the taxonomic affinities between the different species of *Scleromys*/"*Scleromys*" from northern and southern South America remain uncertain, underscoring the importance of a thorough reassessment of the genus. Hence, further cladistic assessments of morphological evidence focused on *Acarechimys* and *Scleromys*/"*Scleromys*" are necessary to analyze such patterns.

These new records reported here contribute to a remarkable glimpse into Miocene biodiversity, with the cooccurrence in this locality of representatives from all four superfamilies: Chinchilloidea (*Neoepiblema* sp., *Potamarchus* sp., *Pseudopotamarchus* sp., cf. "*Scleromys*" sp., and cf. *Microscleromys* sp.), Octodontoidea (*Acarechimys hunikuini*), Erethizontoidea (reported herein), and Cavioidea (*Cardiatherium* sp.) (see Fontoura et al. 2023, 2024; this work). Other Late–Middle Miocene localities also exhibit representatives of these four groups, including, e.g., La Venta (Colombia, 28 taxa; Fields 1957; Walton 1997; Urrea-Barreto et al. 2023) and TAR-31 (Peru, nine taxa; Boivin et al. 2021). The caviomorph fauna from PRE06 shows mixed biochronological affinities, as the identified taxa are individually associated with both Middle and Late Miocene faunas. A similar pattern has been documented for Neogene assemblages from the Fitzcarrald Arch (Peru), which also includes taxa with overlapping Middle and Late Miocene biochronological signals (Antoine et al. 2007; Tejada-Lara et al. 2015). According to Tejada-Lara et al. (2015), this pattern reflects typical features of tropical faunas, such as high taxonomic diversity, stable and long-lasting environmental conditions, and the extended persistence of lineages with broad geographic distributions, a trend particularly evident among rodents (Jablonski et al. 2006). Nevertheless, considering the depositional environment of the fossil-bearing beds, some faunal elements may represent reworked material derived from older sediments. Further studies are required to properly assess this possibility, and ongoing radioisotopic dating analyses of samples from the PRE06 locality are expected to provide a more robust geochronological framework.

Additionally, the faunal similarity between PRE06 and the other Middle–Late Miocene localities mentioned above may be artificial and influenced by methodological bias. The wet or dry screening of sediments in order to collect small-sized fossil remains was employed at PRE06 and TAR-31, for example, but this technique is not always applied in every fossiliferous locality. This is exemplified by Tejada-Lara et al. (2015), who shows that nearly all rodents recovered from Fitzcarrald Arch (14 out of 17 specimens) were found primarily in the localities where wet screening was conducted (IN-008 and DTC-32, two of the 14 localities). Overall, all the specimens discovered at the PRE06 locality (*Acarechimys hunikuini*, Fontoura et al. 2024; *Neoepiblema* sp., *Potamarchus* sp., cf. *Pseudopotamarchus*, *Cardiatherium* sp., Fontoura et al. 2023; and the taxa described herein) attest to the presence of taxa of smaller size in relation to the standard species size range known in these groups. Small-sized diversity is often underestimated when screen-washing techniques are not used (Walton 1997). Therefore, this may not reflect the actual faunal composition but instead result from hydraulic sorting during deposition and/or sampling bias (Battista and Schultz 2024).

The PRE06 "Coqueiros" shares four rodents (genera) with the Middle Miocene Fitzcarrald Arch (*Scleromys*, reported herein; *Potamarchus*, *Neoepiblema*, Fontoura et al. 2023; and *Acarechimys*, Fontoura et al. 2024). It shares three taxa with the Middle Miocene La Venta (*Scleromys*, *Microscleromys*, reported herein, and *Acarechimys*), as well as with the Upper Miocene Patos locality (Acre River; *Potamarchus*, *Neoepiblema*, and *Cardiatherium*), the Cachoeira do Bandeira locality (Acre River; *Pseudopotamarchus*, *Neoepiblema*, and *Cardiatherium*), and Entre Rios ("Conglomerado Osífero"; *Potamarchus*, *Neoepiblema*, and *Cardiatherium*). PRE06 also shares two rodents with the upper Middle Miocene locality TAR-31 (*Scleromys* and *Microscleromys*), and with the Upper Miocene localities CTA-43, CTA-75 (*Potamarchus* and *Acarechimys*), Talismã, Niterói, Morro do Careca, Urumaco, and CTA-44 (*Potamarchus* and *Neoepiblema*). Finally, it shares one taxon with PRJ 28 (Juruá River; *Scleromys*), the Upper Miocene localities CTA-10 (*Neoepiblema*), Río Negro and Puerto Madryn formations (*Cardiatherium*), and the Middle Miocene localities Madre de Díos (*Scleromys*), Quebrada Honda and Collon Curá (*Acarechimys*).

The faunal similarity with Middle Miocene localities such as La Venta, TAR-31 and the Fitzcarrald Arch, and with the Upper Miocene localities such as Acre River and Entre Rios ("Conglomerado Osífero"), further supports the interpretation that the Envira River deposits (PRE06) likely date from the transition between the Middle Miocene, during

the Pebas phase (~16–11.3 Ma; the peak of the Pebas Mega-Wetland System, with lake-embayment and swamp systems reaching their greatest extent; Hoorn et al. 2010), and the Late Miocene, during the Acre phase (~11.3–7 Ma), when this wetland system evolved into a complex environment where deltaic, estuarine and fluvial systems coexisted (Hoorn et al. 2010). This similarity suggests a strong biogeographical connection amid the low-latitude region, also due to similar humid climate associated with the occurrence of rainforests (attributed to the presence of more stable conditions, see the hypothesis of "cradle and museums"; Carrillo-Briceño et al. 2021; Vucetich et al. 2010a), which have been established in Proto-Amazonia since at least the Middle Miocene (Tejada-Lara et al. 2015; Marivaux et al. 2020). Based on this interpretation, associated with the distribution of other specimens between southern and northern South America, in both directions (such as *Acarechimys*, Fontoura et al. 2024; and *Paralonchothrix*, Piñero et al. 2021a), it can be suggested that the Andean Cordillera—whose uplift only began to directly influence the Amazonian landscape from the late Paleogene onward (Hoorn et al. 2010)—did not constitute an overwhelming barrier to mammal dispersals during the Early and Late Miocene in low-latitude lowlands (Croft 2007; Upham et al. 2013; Marivaux et al. 2016, 2020; Boivin et al. 2021; Piñero et al. 2021a; Stutz et al. 2022, 2023).

It is more likely that environmental (e.g., cooler temperatures, increased aridity and establishment of seasonal to semiarid environments in the south; Blisniuk et al. 2005; Pérez et al. 2018; Stutz et al. 2022) and/or geographic barriers influenced the segregation of Northern (Venezuela, Colombia, Peru, western Brazil, and northern Bolivia) from Southern (southern Bolivia, Chile, and Argentina) South America. This resulted in northern faunal assemblages associated with a heterogeneous ecological setting, combining humid forests and open environments, which persisted during the Middle and early Late Miocene (Walton 1997; Antoine et al. 2007; Tejada-Lara et al. 2015; Marivaux et al. 2020; Boivin et al. 2021; Stutz et al. 2022). Thus, in this case the environmental and/or geographical barriers appear to have played a more significant role than time itself (see Tejada-Lara et al. 2015). With the peak of the Andean uplift and the disappearance of the Pebas Mega-Wetland System during the Late Miocene, the Acre System likely acted as a biogeographical corridor, reconnecting continental areas that had previously been isolated (Tejada-Lara et al. 2015; Marivaux et al. 2016).

Conclusions

New species of Erethizontoidea, *Micronoamys candelae* Fontoura gen. et sp. nov., *Enviramys nasifae* Fontoura gen. et sp. nov., and *E. vucetichae* Fontoura gen. et sp. nov. are described from Upper Miocene deposits cropping out in the Envira River, State of Acre, Brazil (Western Amazonia), although the now-enhanced fossil assemblage suggests a potentially older age, it possibly corresponds to the early Late Miocene (as proposed by Fontoura et al. 2023, 2024 and Stutz et al. 2023). The analysed material consists of specimens that are exceptionally small and can only be recovered using sediment screening techniques. These records, which represent an assemblage with some of the smallest Miocene caviomorph rodents (except for *Acarechimys minutissimus*; Arnal et al. 2017) and the smallest Miocene erethizontoids, underscore the coexistence of several caviomorph superfamilies (octodontoids, chinchilloids, and cavioids; see Fontoura et al. 2023, 2024), including now the erethizontoids, at the PRE06 locality. This rich fossiliferous content also includes marsupials (Stutz et al. 2023), fishes (Jacó et al. 2024), rays (Da Silva et al. 2024), dasypodids, birds, and others that are currently under study. This highlights the existence of a rich fauna in Brazilian Amazonia during the Miocene, as in Colombia (La Venta) and Peru (e.g., Contamana and Tarapoto TAR-31). These new records highlight the pivotal role of the Brazilian Amazonian faunas in refining our understanding of Miocene mammalian biogeography in South America, emphasizing the PRE06 locality as a key site for investigating the small vertebrate communities that inhabited Proto-Amazonia prior to the major environmental shifts in South America associated with the rise of the Andes and the global temperature drop over Late Neogene times, prior to the Great American Biotic Interchange. As we have shown, computed tomography represents a valuable tool for assessing virtual tooth wear, an essential method in paleontological studies, particularly when complete specimens representing all ontogenetic stages are lacking. The application of this technique facilitates taxonomic identification, mainly for isolated teeth, enabling an assessment of wear estimation and the observation of structures that were not visible in occlusal view. It enables the comparison of specimens exhibiting different degrees of tooth wear, in both hypsodont (e.g., Skandalos and van den Hoek Ostende 2023) and brachydont form, as demonstrated by Fontoura et al. (2024) and here.

Acknowledgements

We would like to thank everyone who helped in the field trips and who were essential for this research, in particular the colleagues Andrés Alvim and Roberto Ventura Santos (both Universidade Federal de Brasília, Brasilia, Brazil); François Pujos (Instituto Argentino de Nivología, Glaciología y Ciencias Ambientales, CONICET, Mendoza, Argentina); Kathellen G. Magalhães (UFAC); Fernanda Oliveira, Letícia Pales, Nicole Souza, and Tiago Jacó (all Universidade Federal do Rio Grande do Sul, Rio Grande do Sul, Brazil). In addition, we would also like to thank the Pessoa family (Feijó, State of Acre, Brazil), who made their homes available for our camps and other support. Thanks to Agustín G. Martinelli (MACNBR-Museo Argentino de Ciencias Naturales "Bernardino Rivadavia", Buenos Aires, Argentina), Susana Bargo (MLP), Analía A. Rivero and Sonia A. González Patagua (both IDGyM-Instituto de Geología y Minería, Jujuy, Argentina), Alicia Álvarez and Marcos D. Ercoli (both INECOA-Instituto de Ecorregiones Andinas, IDGyM, Jujuy, Argentina) for providing access to specimens under their care. Gratitude is extended to Alba Ramirez (IDGyM), Liliana

C. Lupo (INECOA), Alicia Álvarez (INECOA, IDGyM), Marcos D. Ercoli (INECOA, IDGyM), the Consejo Asesor IDGyM (specially Javier Elortegui Palacios and Guadalupe Maro), the Subsecretaría de Cooperación Internacional and the Universidad de Jujuy for their support and cooperation in facilitating the development of this article, as well as for kindly receiving EF at their facilities. Thanks to Conselho Nacional de Desenvolvimento Científico e Tecnológico (CNPq) and Fundação de Amparo à Pesquisa do Estado do Rio Grande do Sul for the support. We extend our gratitude to Cibele Lima Florence and William da Silveira Freitas (both Institute of Petroleum and Natural Resources, Porto Alegre, Brazil) for µCT-scan acquisitions and treatments. We are grateful to Felipe Busker (IPGP-Instituto Patagónico de Geología y Paleontología, Puerto Madryn, Argentina), Michelle Arnal (Universidad Nacional de La Plata, La Plata, Argentina), and Alejandro G. Kramarz (MACNBR), and the reviewers Lawrence Flynn (Harvard University, Cambridge, USA) and Pedro Piñero (Universitat de València, València, Spain) for their insightful comments, which significantly contributed to improving the manuscript. EF is supported by the Conselho Nacional de Desenvolvimento Científico e Tecnológico (CNPq), 140639/2021-7; 172571/2025-1 and Fundação de Amparo à Pesquisa do Estado do Rio Grande do Sul (FAPERGS), 24/2551-0001745-3. LK is supported by CNPq 309178/2022-3, 406902/2022-4; FAPERGS 21/2551-0002030-0. LM and POA were supported by the French Agence Nationale de la Recherche ("Investissements d'Avenir" grant LabEx CEBA, ANR-10-LABX-25-01) and the Coordenação de Aperfeiçoamento de Pessoal de Nível Superior (CAPES, COFECUB program Te 924/18 "Paléo-Amazone: evolution néogène de l'Amazonie Brésilienne", 88881.143095/2017-01). AMR is supported by CNPq PQ/310023/2021-1/PQ, Protax/441626/2020-3, FAPERGS 21/2551-0000781-8; 445906/2024-3, FAPERGS 25/2551-0001737-8.

Editor: Eudald Mujal Grané

References

Agassiz, L. and Agassiz, E. 1868. *A Journey in Brazil.* 540 pp. Ticknor and Fields, Boston.

Álvarez, A., Arévalo, R.L., and Verzi, D.H. 2017. Diversification patterns and size evolution in caviomorph rodents. *Biological Journal of the Linnean Society* 121: 907–922.

Ameghino, F. 1887. Enumeración sistemática de las especies de mamíferos fósiles coleccionados por Carlos Ameghino en los terrenos eocenos de Patagonia austral y depositados en el museo de La Plata. *Boletín del Museo de La Plata* 1: 1–26.

Ameghino, F. 1899. *Sinopsis geológico-paleontológica. Suplemento (adiciones y corecciones)*. 13 pp. La Libertad, La Plata.

Ameghino, F. 1894. Énumération synoptique des espèces de mammifères fossiles des formations éocènes de Patagonie. *Boletin de la Academia Nacional de Ciencias en Córdoba* 13: 259–455.

Anthony, H.E. 1922. A new fossil rodent from Ecuador. *American Museum Novitates* 35: 1–4.

Antoine, P.-O., Abello, M., Adnet, S., Altamirano Sierra, A.J., Baby, P., Billet, G., Boivin, M., Calderón, Y., Candela, A., Chabain, J., Corfu, F., Croft, D.A., Ganerød, M., Jaramillo, C., Klaus, S., Marivaux, L., Navarrete, R.E., Orliac, M.J., Parra, F., Pérez, M.E., Pujos, F., Rage, J.C., Ravel, A., Robinet, C., Roddaz, M., Tejada-Lara, J.V., Vélez Juarbe, J., Wesselingh, F.P., and Salas-Gismondi, R. 2016. A 60-million-year Cenozoic history of western Amazonian ecosystems in Contamana, eastern Peru. *Gondwana Research* 31: 30–59.

Antoine, P.-O., Marivaux, L., Croft, D.A., Billet, G., Ganerød, M., Jaramillo, C., Martin, T., Orliac, M.J., Tejeda, J., Altamirano, A.J., Duranthon, F., Fanjat, G., Rousse, S., and Salas Gismondi, R. 2012. Middle Eocene rodents from Peruvian Amazonia reveal the pattern and timing of caviomorph origin and biogeography. *Proceedings of the Royal Society B: Biological Sciences* 279: 1319–1326.

Antoine, P.-O., Roddaz, M., Brichau, S., Louterbach, M., Salas Gismondi, R., Altamirano, A., Tejada, J., Lambs, L., Otto, T., and Brusset, S. 2013. Middle Miocene vertebrates from the Amazonian Madre de Dios Subandean Zone, Peru. *Journal of South American Earth Sciences* 42: 91–102.

Antoine, P.-O., Salas-Gismondi, R., Baby, P., Benammi, M., Brusset, S., De Franceschi, D., Espurt, N., Goillot, C., Pujos, F., Salas-Gismondi, R., Tejada, J., and Urbina, M. 2007. The middle Miocene (Laventan) Fitzcarrald fauna, Amazonian Peru. Fourth European Meeting on the Paleontology and Stratigraphy of Latin America, Madrid, España. *Cuadernos del Museo Geominero* 8: 355–360.

Arnal, M. and Kramarz, A.G. 2011. First complete skull of an octodontoid (Rodentia, Caviomorpha) from the Early Miocene of South America and its bearing in the early evolution of Octodontoidea. *Geobios* 44: 435–444.

Arnal, M. and Pérez, M.E. 2013. A new acaremyid rodent (Hystricognathi: Octodontoidea) from the Middle Miocene of Patagonia (South America) and considerations on the early evolution of Octodontoidea. *Zootaxa* 3616: 119–134.

Arnal, M. and Vucetich, M.G. 2014. Revision of the fossil rodent *Acaremys* Ameghino, 1887 (Hystricognathi, Octodontoidea, Acaremyidae) from the Miocene of Patagonia (Argentina) and the description of a new acaremyid. *Historical Biology* 27: 42–59.

Arnal, M., Kramarz, A.G., Vucetich, M.G., Frailey, C.D., and Campbell, K.E. 2020. New Palaeogene caviomorphs (Rodentia, Hystricognathi) from Santa Rosa, Peru: systematics, biochronology, biogeography and early evolutionary trends. *Papers in Palaeontology* 6: 193–216.

Arnal, M., Pérez, M.E., and Deschamps, C. 2019. Revision of the Miocene caviomorph rodents from the Rio Santa Cruz (Argentinean Patagonia). *Publicación Electrónica de la Asociación Paleontológica Argentina* 19: 193–229.

Arnal, M., Pérez, M.E., Tejada, L.M., and Campbell, K.E. 2022. The high taxonomic diversity of the Palaeogene hystricognath rodents (Caviomorpha) from Santa Rosa (Peru, South America) framed within a new geochronological context. *Historical Biology* 34: 2350–2373.

Arnal, M., Vucetich, M.G., Croft, D.A., Bargo, M.S., Fernicola, J.C., and Vizcaino, S.F. 2017. Systematic revision and evolutionary history of *Acarechimys* Patterson in Kraglievich, 1965 (Rodentia, Caviomorpha, Octodontoidea). *Ameghiniana* 54: 307–330.

Assemat, A., Boivin, M., Marivaux, L., Pujos, F., Benites-Palomino, A., Salas-Gismondi, R., Tejada-Lara, J. V., Varas-Malca, R.M., Negri, F.R., Ribeiro, A.M., and Antoine, P.-O. 2019. Restes inédits de rongeurs caviomorphes du Paléogène de la région de Juanjui (Amazonie péruvienne): systématique, implications macro-évolutives et biostratigraphiques. *Geodiversitas* 41: 699–730.

Battista, F. and Schultz, C.L. 2024. Sampling and collector biases as taphonomic filters: an overview. *Anais da Academia Brasileira de Ciências* 96 (4): e20231242.

Bergqvist, L.P., Ribeiro, A.M., and Bocquentin-Villanueva, J. 1998. Primata, roedores e litopternas do Mio-Plioceno da Amazônia Sul-Ocidental (Formação Solimões, Bacia do Acre), Brasil. *Geología Colombiana* 23: 19–29.

Bertrand, O.C., Flynn, J.J., Croft, D.A., and Wyss, A.R. 2012. Two new taxa (Caviomorpha, Rodentia) from the Early Oligocene Tinguiririca fauna (Chile). *American Museum Novitates* 3750: 1–36.

Bissaro-Júnior, M.C., Kerber, L., Crowley, J.L., Ribeiro, A.M., Ghilardi, R.P., Guilherme, E., Negri, F.R., Souza Filho, J.P., and Hsiou, A.S. 2019. Detrital zircon U-Pb geochronology constrains the age of Brazilian Neogene deposits from Western Amazonia. *Palaeogeography, Palaeoclimatology, Palaeoecology* 16: 64–70.

Blisniuk, P.M., Stern, L.A., Page Chamberlain, C., Idleman, B., and Zeitler, P.K. 2005. Climatic and ecologic changes during Miocene surface uplift in the southern Patagonian Andes. *Earth and Planetary Science Letters* 230: 125–142.

Boivin, M., and Marivaux, L. 2020. Dental homologies and evolutionary transformations in Caviomorpha (Hystricognathi, Rodentia): new data

from the Paleogene of Peruvian Amazonia. *Historical Biology* 32: 528–554.

Boivin, M., Ginot, S., Marivaux, L., Altamirano-Sierra, A.J., Pujos, F., Salas-Gismondi, R., Tejada-Lara, J.V., and Antoine, P.-O. 2019. Tarsal morphology and locomotor adaptation of some late middle Eocene caviomorph rodents from Peruvian Amazonia reveal early ecological diversity. *Journal of Vertebrate Paleontology* 38 (6): e1555164.

Boivin, M., Marivaux, L., Aguirre-Diaz, W., Andriolli Custódio, M., Benites-Palomino, A., Pujos, F., and Antoine, P.-O. 2022. Eocene caviomorph rodents from Balsayacu (Peruvian Amazonia). *Paläontologische Zeitschrift* 96: 135–160.

Boivin, M., Marivaux, L., Aguirre-Diaz, W., Benites-Palomino, A., Billet, G., Pujos, F., Salas-Gismondi, R., Stutz, N.S., Tejada-Lara, J.V., Varas-Malca, R.M., Walton, A.H., and Antoine, P.-O. 2021. Late middle Miocene caviomorph rodents from Tarapoto, Peruvian Amazonia. *PLoS ONE* 16 (11): e0258455.

Boivin, M., Marivaux, L., Candela, A.M., Orliac, M.J., Pujos, F., Salas-Gismondi, R., Tejada-Lara, J.V., and Antoine, P.-O. 2017a. Late Oligocene caviomorph rodents from Contamana, Peruvian Amazonia. *Papers in Palaeontology* 3: 69–109.

Boivin, M., Marivaux, L., Orliac, M.J., Pujos, F., Salas-Gismondi, R., Tejada-Lara, J.V., and Antoine, P.-O. 2017b. Late middle Eocene caviomorph rodents from Contamana, Peruvian Amazonia. *Palaeontologia Electronica* 20.1.19A: 1–50.

Boivin, M., Marivaux, L., Pujos, F., Salas-Gismondi, R., Tejada-Lara, J.V., Varas-Malca, R.M., and Antoine, P.-O. 2018. Early Oligocene caviomorph rodents from Shapaja, Peruvian Amazonia. *Palaeontographica Abteilung A* 311 (1–6): 87–156.

Buffan, L., Condamine, F.L., Stutz, N.S., Pujos, F., Antoine, P.-O., and Marivaux, L., 2025. The fate of South America's endemic mammal fauna in response to the most dramatic Cenozoic climate disruption. *Proceedings of the National Academy of Sciences of the United States of America* 122 (20): e2419520122.

Busker, F. and Dozo, M.T. 2017. First confirmed record of *Incamys bolivianus* (Caviomorpha, Chinchilloidea) in the Deseadan of Patagonia (Argentina). *Ameghiniana* 54: 706–712.

Busker, F., Pérez, M.E., and Dozo, M.T. 2019. A new chinchilloid (Rodentia, Hystricognathi) from the early Miocene of the localities of Bryn Gwyn and Gran Barranca (Patagonia, Argentina). *Comptes Rendus Palevol* 18: 525–540.

Calandra, I., Labonne, G., Schulz-Kornas, E., Kaiser, T.M., and Montuire, S. 2016. Tooth wear as a means to quantify intra-specific variations in diet and chewing movements. *Scientific Reports* 6: 34037.

Campbell, K.E. Jr., Frailey, C.D., and Romero-Pittman, L. 2006. The Pan-Amazonian Ucayali Peneplain, late Neogene sedimentation in Amazonia, and the birth of the modern Amazon River system. *Palaeogeography, Palaeoclimatology, Palaeoecology* 239: 166–219.

Candela, A.M. 1999. The evolution of the molar pattern of the Erethizontidae (Rodentia, Hystricognathi) and the validity of *Parasteiromys* Ameghino, 1904. *Palaeovertebrata* 28: 53–73.

Candela, A.M. 2000. *Los Erethizontidae (Rodentia, Hystricognathi) fósiles de Argentina. Sistemática e historia evolutiva y biogeográfica*. 352 pp. Ph.D. Thesis, Facultad de Ciencias Naturales y Museo de La Plata, La Plata.

Candela, A.M. 2002. Lower deciduous tooth homologies in Erethizontidae (Rodentia, Hystricognathi): Evolutionary significance. *Acta Palaeontologica Polonica* 47: 717–723.

Candela, A.M. 2003. A new porcupine (Rodentia, Erethizontidae) from the early and middle Miocene of Patagonia. *Ameghiniana* 40: 483–494.

Candela, A.M. 2004. A new giant porcupine (Rodentia, Erethizontidae) from the late Miocene of Argentina. *Journal of Vertebrate Paleontology* 24: 732–741.

Candela, A.M. and Nasif, N.L. 2006. Systematics and biogeographic significance of *Drytomomys typicus* (Scalabrini in Ameghino, 1889) nov. comb., a Miocene Dinomyidae (Rodentia, Hystricognathi) from Northeast of Argentina. *Neues Jahrbuch für Geologie und Paläontologie Monaschefte* 2006 (3): 165–181.

Candela, A.M., Galli, C.I., Rasia, L.L., Voglino, D., Abello, M.A., García Esponda, C.M., and Zurita, A.E. 2021. Late Miocene mammals from the Calchaquí Valley (Palo Pintado Formation, northwestern Argentina): Biogeographic and paleoenvironmental implications for the southern central Andes. *Journal of South American Earth Sciences* 112: 103602.

Carrillo, J.D. and Sánchez-Villagra, M.R. 2015. Giant rodents from the Neotropics: diversity and dental variation of late Miocene neoepiblemid remains from Urumaco, Venezuela. *Palaontologische Zeitschrift* 89: 1057–1071.

Carrillo, J.D., Jaramillo, C., Abadía, F., Aguilera, O., Alfonso-Rojas, A., Billet, G., Benites-Palomino, A., Cadena, E.-A., Cárdenas, A., Carlini, A.A., Carrillo-Briceño, J., Carvalho, M., Cortés, D., Escobar, J., Herrera, F., Link, A., Luque, J., Martínez, C., Pérez-Lara, D.K., Salas-Gismondi, R., Suarez, C., Stiles, E., Urrea-Barreto, F.J., and Zapata, S. 2023. The Miocene La Venta Biome (Colombia): A century of research and future perspectives. *Geodiversitas* 45: 739–767.

Carrillo-Briceño, J.D., Sánchez, R., Scheyer, T.M., Carrillo, J.D., Delfino, M., Georgalis, G.L., Kerber, L., Ruiz-Ramoni, D., Birindelli, J.L.O., Cadena, E.-A., Rincón, A.F., ChavezHoffmeister, M., Carlini, A.A., Carvalho, M.R., Trejos-Tamayo, R., Vallejo, F., Jaramillo, C., Jones, D.S., and Sánchez-Villagra, M.R. 2021. A Pliocene–Pleistocene continental biota from Venezuela. *Swiss Journal of Palaeontology* 140: art. 9.

Cerdeño, E. and Vucetich, M.G. 2007. The first rodent from the Mariño Formation (Miocene) at Divisadero Largo (Mendoza, Argentina) and its biochronological implications. *Andean Geology* 34: 199–207.

Chandless, W. 1866. Ascent of the River Purûs. *Journal of the Royal Geographical Society of London* 36: 86–118.

Cozzuol, M.A. 2006. The Acre vertebrate fauna: Age, diversity, and geography. *Journal of South American Earth Sciences* 21: 185–203.

Croft, D.A. 2007. The middle Miocene (Laventan) Quebrada Honda fauna, southern Bolivia and a description of its notoungulates. *Palaeontology* 50: 277–303.

Croft, D.A., Chick, J.M., and Anaya, F. 2011. New Middle Miocene caviomorph rodents from Quebrada Honda, Bolivia. *Journal of Mammalian Evolution* 18: 245–268.

Croft, D.A., Flynn, J.J., Wyss, A.R., Charrier, R., and Anaya, F. 2021. New chinchillid rodents (Hystricognathi: Caviomorpha) from northern Chile and Bolivia fill a 17-million-year gap in the pan-chinchilline fossil record. *Journal of Mammalian Evolution* 28: 1205–1236.

Da Silva, H.C., Ferigolo, J., Negri, F.R., Jacó, T.R.F., Ribeiro, A.M., and Reis, R.E. 2024. Deformidades dentárias de arraias Potamotrygonidae do Acre, Mioceno da Formação Solimões (Bacia do Acre), Brasil. *In*: C.S. Scherer, D.H. Oliveira, M.C. Silva, M.A.T. Dantas, R.V.C. Araripe, R.R.C. Duque, and Y. Asakura (eds.), *Paleodest – Paleontologia em Destaque*, 316–316. Sociedade Brasileira de Paleontologia, Maceió.

Deschamps, C.M. and Tomassini, R.L. 2016. Late Cenozoic vertebrates from the southern Pampean Region: systematic and bio-chronostratigraphic update. *In*: M. Martínez and D. Olivera (eds.), Palinología del MesoCenozoico de Argentina – Volumen en homenaje a Mirta Elena Quattrocchio. *Publicación Electrónica de la Asociación Paleontológica Argentina* 16: 202–225.

Dozo, M.T., Vucetich, M.G., and Candela, A.M. 2004. Skull anatomy and neuromorphology of *Hypsosteiromys*, a Colhuehuapian erethizontid rodent from Argentina. *Journal of Vertebrate Paleontology* 24: 228–234.

Ercoli, M.D., Álvarez, A., Verzi, D.H., Villalba Ulberich, J.P., Quiñones, S.I., Constantini, O.E., and Zurita, A.E. 2021. A new mammalian assemblage for Guanaco Formation (northwestern Argentina), and the description of a new genus of New World porcupine. *Journal of South American Earth Sciences* 110: 103389.

Esteban, G.I., Nasif, N., and Georgieff, S.M. 2014. Cronobioestratigrafía del Mioceno tardío-Plioceno temprano, Puerta de Corral Quemado y Villavil, provincia de Catamarca, Argentina. *Acta Geológica Lilloana* 26: 165–192.

Fedorov, A., Beichel, R., Kalpathy-Cramer, J., Finet, J., Fillion-Robin, J.C., Pujol, S., Bauer, C., Jennings, D., Fennessy, F., Sonka, M., Buatti, J., Aylward, S., Miller, J.V., Pieper, S., and Kikinis, R. 2012. 3D

Slicer as an image computing platform for the Quantitative Imaging Network. *Magnetic Resonance Imaging* 30: 1323–1341.

Ferigolo, J. 2025. *Glossário etmológico de vertebrados: Origem grega e Latina dos termos*. 456 pp. Editora Appris, Curitiba.

Fields, R.W. 1957. Hystricomorph rodents from the late Miocene of Colombia, South America. *University of California Publications in Geological Sciences* 32: 273–404.

Flynn, J.J., Charrier, R., Croft, D.A., Gans, P.B., Herriott, T.M., Wertheim, J.A., and Wyss, A.R. 2008. Chronologic implications of new Miocene mammals from the Cura-Mallín and Trapa Trapa formations, Laguna del Laja area, south central Chile. *Journal of South American Earth Sciences* 26: 412–423.

Flynn, J.J., Novacek, M.J., Dodson, H.E., Frassinetti, D., McKenna, M.C., Norell, M.A., Sears, K.E., Swisher, C.C. and Wyss A.R. 2002. A new fossil mammal assemblage from the southern Chilean Andes: implications for geology, geochronology, and tectonics. *Journal of South American Earth Sciences* 15: 285–302.

Fontoura, E., Boivin, M., Marivaux, L., Antoine, P.-O., Stutz, N.S., Negri, F.R., Ribeiro, A.M., and Kerber, L. 2024. A new Late Miocene stem Octodontoid (Rodentia: Caviomorpha: Octochinchilloi) from the Solimões Formation (Brazil): paleobiogeographic implications. *Journal of Vertebrate Paleontology* 44 (1): e2382822.

Fontoura, E., Negri, F.R., Ribeiro, A.M., and Kerber, L. 2023. A new Late Miocene hystricognath rodent assemblage (Caviidae, Dinomyidae, and Neoepiblemidae) from northern Brazil and its biostratigraphic relevance. *Historical Biology* 35: 2094–2104.

Frailey, C.D. 1986. Late Miocene and Holocene mammals, exclusive of the Notoungulata, of the Rio Acre region, western Amazonia. *Los Angeles County Museum Contributions in Science* 374: 1–46.

Frailey, C.D. and Campbell, K.E. 2004. Paleogene rodents from Amazonian Peru: The Santa Rosa local fauna. *In*: K.E. Campbell (ed.), The Paleogene Mammalian Fauna of Santa Rosa, Amazonian Peru. *Natural History Museum of Los Angeles County, Science Series* 40: 71–130

Hoorn, C., Wesselingh, F.P., Hovikoski, J., and Guerrero, J. 2010. The development of the Amazonian mega-wetland (Miocene; Brazil, Colombia, Peru, Bolivia). *In*: C. Hoorn and F.P. Wesselingh (eds.), *Amazonia, Landscape and Species Evolution*, 123–142. Blackwell Publishing Ltd., Chichester.

Hsiou, A.S., Bissaro-Junior, M.C., Muniz, F.P., Negri, F.R., Ribeiro, A.M., and Kerber, L. 2022. Bacia do Acre: evidências das paisagens da proto-Amazônia há 10 milhões de anos, com base em vertebrados fósseis da Formação Solimões. *In*: L. Corecco (ed.), *Paleontologia do Brasil: Paleoecologia e Paleoambientes*, 29–64. Editora Interciência, Rio de Janeiro.

ICZN 2012. *International Code of Zoological Nomenclature*. Consolidated 4th edition. Available from: https://www.iczn.org/the-code/ [accessed: 15/04/2025].

Jablonski, D. 2008. Extinction and the spatial dynamics of biodiversity. *Proceedings of the National Academy of Sciences* 105: 11528–11535.

Jablonski, D., Roy, K., and Valentine, J.W. 2006. Out of the tropics: evolutionary dynamics of the latitudinal diversity gradient. *Science* 314: 102–106.

Jacó, T.R.F., da Silva, H.C., Boneberg, M., Negri, F.R., and Ribeiro, A.M. 2024. A paleoictiofauna da localidade Coqueiros (Formação Solimões), Rio Envira, Acre, Brasil. *In*: C.S. Scherer, D.H. Oliveira, M.C. Silva, M.A.T. Dantas, R.V.C. Araripe, R.R.C. Duque, and Y. Asakura (eds.), *Paleodest – Paleontologia em Destaque*, 331–331. Sociedade Brasileira de Paleontologia, Maceió.

Janis, C.M. 1986. An estimation of tooth volume and hypsodonty indices in ungulate mammals, and the correlation of these factors with dietary preference. *In*: D.E. Russell, J.P. Santoro and D. Sigogneau-Russell (eds.), Teeth Revisited. Proceedings of the 7th International Symposium on Dental Morphology. *Mémoires du Muséum national d'histoire naturelle, Série C, Paris* 53: 367–387.

Kay, R.F. and Cozzuol, M.A. 2006. New platyrrhine monkeys from the Solimões Formation (late Miocene, Acre State, Brazil). *Journal of Human Evolution* 50: 673–686.

Kay, R.F. and Frailey, C.D. 1993. Large fossil platyrrhines from the Río Acre local fauna, late Miocene, western Amazonia. *Journal of Human Evolution* 25: 319–327.

Kerber, L. 2017. Imigrantes em um continente perdido: O registro fossilifero de roedores Caviomorpha (Mammalia: Rodentia: Ctenohystrica) do Cenozoico do Brasil. *Terrae Didática* 13: 185–211.

Kerber, L., Bissaro-Júnior, M.C., Negri, F.R., de Souza-Filho, J.P., Guilherme, E., and Hsiou, A.S. 2017a. A new rodent (Caviomorpha: Dinomyidae) from the upper Miocene of southwestern Brazilian Amazonia. *Historical Biology* 30: 985–993.

Kerber, L., Mayer, L.M., Gomes, A.C., and Nasif, N. 2018a. On the morphological, taxonomic, and phylogenetic status of South American Quaternary dinomyid rodents (Rodentia: Dinomyidae). *Paläontologische Zeitschrift* 94: 167–178.

Kerber, L., Negri, F.R., and Sanfelice, D. 2018b. Morphology of cheek teeth and dental replacement in the extinct rodent *Neoepiblema* Ameghino, 1889 (Caviomorpha, Chinchilloidea, Neoepiblemidae). *Journal of Vertebrate Paleontology* 38: e1549061-2.

Kerber, L., Negri, F.R., Ferigolo, J., Mayer, E.L., and Ribeiro, A.M. 2017b. Modifications on fossils of neoepiblemids and other South American rodents. *Lethaia* 50: 149–161.

Kerber, L., Negri, F.R., Ribeiro, A.M., Nasif, N., Souza-Filho, J.P., and Ferigolo, J. 2017c. Tropical fossil caviomorph rodents from the southwestern Brazilian Amazonia in the context of the South American faunas: systematics, biochronology, and paleobiogeography. *Journal of Mammalian Evolution* 24: 57–70.

Kerber, L., Negri, F.R., Ribeiro, A.M., Vucetich, M.G., and Souza-Filho, J.P. 2016. Late Miocene potamarchine rodents from southwestern Amazonia, Brazil: with description of new taxa. *Acta Palaeontologica Polonica* 61: 191–203.

Koenigswald, W. 2016. Specialized wear facets and late ontogeny in mammalian dentitions. *Historical Biology* 30: 7–29.

Kramarz, A.G. 2004. Octodontoids and erethizontoids (Rodentia, Hystricognathi) from the Pinturas Formation, Early–Middle Miocene of Patagonia, Argentina. *Ameghiniana* 41: 199–216.

Kramarz, A.G. 2006. *Neoreomys* and *Scleromys* (Rodentia: Hystricognathi) from the Pinturas Formation, late Early Miocene of Patagonia, Argentina. *Revista del Museo Argentino de Ciencias Naturales* 8: 53–62.

Kramarz, A.G. and Bellosi, E.S. 2005. Hystricognath rodents from the Pinturas Formation, early–middle Miocene of Patagonia, biostratigraphic and paleoenvironmental implications. *Journal of South American Earth Sciences* 18: 199–212.

Kramarz, A.G., Bellosi, E.S., Bond, M., Forasiepi, A.M., Fernández, M., Fernicola, J.C., Aguirrezebala, G., and Rezende, D.T. 2025. Uneven landscapes inhabited by middle Miocene mammals from La Pava and Collón Cura formations in North Patagonia. *Swiss Journal of Palaeontology* 144: e26.

Kramarz, A.G., Vucetich, M.G., and Arnal, M. 2013. A new early Miocene chinchilloid hystricognath rodent; an approach to the understanding of the early chinchillid dental evolution. *Journal of Mammalian Evolution* 20: 249–261.

Latrubesse, E.M., da Silva, S.A.F., Cozzuol, M., and Absy, M.L. 2007. Late Miocene continental sedimentation in southwestern Amazonia and its regional significance: Biotic and geological evidence. *Journal of South American Earth Sciences* 23: 61–80.

Lavocat, R. 1976. Rongeurs caviomorphes de l'Oligocène de Bolivie. Rongeurs du bassin déséadien de Salla. *Palaeovertebrata* 7: 15–90.

Mammal Diversity Database 2025. *Mammal Diversity Database* (Version 2.3) Data set. Zenodo. https://doi.org/10.52817/zenodo.17033774

Marivaux, L., Adnet, S., Altamirano-Sierra, A.J., Pujos, F., Ramdarshan, A., Salas-Gismondi, R., Tejada-Lara, J.V., and Antoine, P.-O. 2016. Dental remains of cebid platyrrhines from the earliest late Miocene of Western Amazonia, Peru: macroevolutionary implications on the extant capuchin and marmoset lineages. *American Journal of Physical Anthropology* 161: 478–493.

Marivaux, L., Aguirre-Diaz, W., Benites-Palomino, A., Billet, G., Boivin, M., Pujos, F., Salas-Gismondi, R., Tejada-Lara, J.V., Varas-Malca, R.M., and Antoine, P.-O. 2020. New record of *Neosaimiri* (Cebidae, Platyrrhini) from the late Middle Miocene of Peruvian Amazonia. *Journal of Human Evolution* 146: 102835.

Marivaux, L., Negri, F.R., Antoine, P.-O., Stutz, N.S., Condamine, F.L., Kerber, L., Pujos, F., Ventura Santos, R., Alvim, A.M.V., Hsiou, A.S., Bissaro, M.C., Adami-Rodrigues, K., and Ribeiro, A.M. 2023. An eosimiid primate of South Asian affinities in the Paleogene of Western Amazonia and the origin of New World monkeys. *Proceedings of the National Academy of Sciences of the United States of America* 120 (28): e2301338120.

McGrath, A.J., Chick, J., Croft, D.A., Dodson, H.E., Flynn, J.J., and Wyss, A.R. 2022. Cavioids, Chinchilloids, and Erethizontoids (Hystricognathi, Rodentia, Mammalia) of the Early Miocene Pampa Castillo fauna, Chile. *American Museum Novitates* 2022 (3984): 1–46.

McGrath, A.J., Flynn, J.J., Croft, D.A., Chick, J., Dodson, H.E., and Wyss, A.R. 2023. Caviomorphs (Rodentia, Hystricognathi) from Pampa Castillo, Chile: new octodontoid records and biochronological implications. *Papers in Palaeontology* 9 (1): e1477.

Mones, A. and Toledo, P.M. 1989. Primer hallazgo de *Euphilus* Ameghino, 1889 (Mammalia: Rodentia: Neoepiblemidae) en el Neógeno del estado de Acre, Brasil. *Comunicaciones Paleontologicas Del Museo de Historia Natural de Montevideo* 21 (2): 1–15.

Montalvo, C.I., Tomassini, R.L., Sostillo, R., Cerdeño, E., Verzi, D.H., Visconti, G., Folguera, A., and Schmidt, G.I. 2019. A Chasicoan (late Miocene) vertebrate assemblage from Cerro Azul Formation, central Argentina. Geomorphological and biochronological considerations. *Journal of South American Earth Sciences* 95: 102218.

Muniz, F.P., Bissaro-Júnior, M.C., Guilherme, E., Souza-Filho, J.P., Negri, F.R., and Hsiou A.S. 2021. Vertebrate taphonomy of two upper Miocene bonebeds in Western Proto Amazonia (Solimões Formation, Brazil): Insights from Marcrovertebrate and Microvertebrate Fossils. *Palaios* 36: 269–282.

Muniz, F.P., Bissaro-Júnior, M.C., Guilherme, E., Souza-Filho, J.P., Negri, F.R., and Hsiou A.S. 2022. Fossil frogs from the Upper Miocene of Southwestern Brazilian Amazonia (Solimões Formation, Acre Basin). *Journal of Vertebrate Paleontology* 41: e2089853.

Nasif, N.L., Candela, A.M., Rasia, L., Madozzo-Jaén, M.C., and Bonini, R. 2013. Actualización del conocimiento de los roedores del Mioceno Tardío de la Mesopotamia argentina: aspectos sistemáticos, evolutivos y paleobiogeográficos. *Publicación Electrónica de la Asociación Paleontológica Argentina* 14: 147–163.

Negri, F.R. and Ferigolo, J. 1999. Anatomia craniana de *Neoepiblema ambrosettianus* (Ameghino, 1889) (Rodentia, Caviomorpha, Neoepiblemidae) do Mioceno superior-Plioceno, Estado do Acre, Brasil, e revisão das espécies do gênero. *Boletim do Museu Paraense Emílio Goeldi* 10: 1–80.

Negri, F.R., Bocquentin-Villanueva, J., Ferigolo, J., and Antoine, P.-O. 2010. A Review of Tertiary Mammal Faunas and Birds from Western Amazonia. *In*: C. Hoorn and F. P. Wesselingh (eds.), *Amazonia: Landscape and Species Evolution*, 243–258. Blackwell Publishing Ltd., West Sussex.

Patterson, B. 1942. Two Tertiary mammals from northern South America. *American Museum Novitates* 1173: 1–8.

Patton, J.L., Pardiñas, U.F., and d'Elia, G. 2015. *Mammals of South America*. *Vol. 2: Rodents*. 384 pp. University of Chicago Press, Chicago.

Paula Couto, C. 1978. Fossil mammals from the Cenozoic of Acre, Brazil. 2. Rodentia Caviomorpha Dinomyidae. *Iheringia – Série Geologia* 5: 3–17.

Paula Couto, C. 1983. Fossil mammals from the Cenozoic of Acre, Brazil. 5. Miscellanea. *Iheringia, Série Geologia* 8: 101–108.

Perea, D., Corona, A., Ubilla, M., Manzuetti, A., Badín, A.C., Montenegro, F., Toriño, P., and Rinderknecht, A. 2023. The Camacho Formation of Uruguay (Late Miocene): New vertebrate findings, biostratigraphic update, associated environments, and chronostratigraphic remarks. *Journal of South American Earth Sciences* 130: 104585.

Pérez, M.E., Arnal, M., Boivin, M., Vucetich, M.G., Candela, A., Busker, F., and Mamani Quispe, B. 2018. New caviomorph rodents from the late Oligocene of Salla, Bolivia: taxonomic, chronological, and biogeographic implications for the Deseadan faunas of South America. *Journal of Systematic Palaeontology* 17: 821–847.

Piñero, P., Olivares, A.I., Verzi, D.H., and Contreras, V.H. 2021a. *Paralonchothrix* gen. nov., the first record of Echimyini (Rodentia, Octodontoidea) in the late Miocene of Southern South America. *Earth and Environmental Science Transactions of the Royal Society of Edinburgh* 112: 147–158.

Piñero, P., Verzi, D.H., Olivares, A.I., Montalvo, C.I., Tomassini, R.L., and Villoldo, A.F. 2021b. Evolutionary pattern of *Metacaremys* gen. nov. (Rodentia, Octodontidae) and its biochronological implications for the late Miocene and early Pliocene of southern South America. *Papers in Palaeontology* 7: 1895–1917.

Rasia, L.L. and Candela, A.M. 2019. Upper molar morphology, homologies and evolutionary patterns of chinchilloid rodents (Mammalia, Caviomorpha). *Journal of Anatomy* 234: 50–65.

Rasia, L.L., Candela, A.M., and Cañón, C. 2021. Comprehensive total evidence phylogeny of chinchillids (Rodentia, Caviomorpha): Cheek teeth anatomy and evolution. *Journal of Anatomy* 239: 405–423.

Ribeiro, A.M., Madden, R.H., Negri, F.R., Kerber, L., Hsiou, A.S., and Rodrigues, K.A. 2013. Mamíferos fósiles y biocronología en el suroeste de la Amazonia, Brasil. *In:* D. Brandoni and J.I. Noriega (eds.), El Neógeno de la Mesopotamia Argentina. *Asociación Paleontológica Argentina, Publicación Especial* 14: 207–221.

Rinderknecht, A., Bostelmann, E., and Ubilla, M. 2017. Making a giant rodent: cranial anatomy and ontogenetic development in the genus *Isostylomys* (Mammalia, Hystricognathi, Dinomyidae). *Journal of Systematic Palaeontology* 16: 245–261.

Robinet, C., Merceron, G., Candela, A.M., and Marivaux, L. 2020. Dental microwear texture analysis and diet in extant caviomorphs (Rodentia) from the Serra do Mar Atlantic forest ecoregion (Brazil). *Journal of Mammalogy* 101: 386–402.

Robinet, C., Merceron, G., Candela, A.M., and Marivaux, L. 2025. Del diente a la dieta: modelo de interpretación del microdesgaste dentario en roedores caviomorfos actuales. *Boletim Informativo da Sociedade Brasileira de Paleontologia* 40 (83): 27–84.

Robinet, C., Merceron, G., Catzeflis, F., Candela, A.M., and Marivaux, L. 2022. About inter- and intra-specific variability of dental microwear texture in rodents: study of two sympatric *Proechimys* (Echimyidae) species from the Cacao locality, French Guiana. *Palaeogeography, Palaeoclimatology, Palaeoecology* 591: 110880.

Rowe, D.L. and Honeycutt, R.L. 2002. Phylogenetic relationships, ecological correlates, and molecular evolution within the Cavioidea (Mammalia, Rodentia). *Molecular Biology and Evolution* 19: 263–277.

Sant'Anna-Filho, M.J. 1994. *Roedores do Neógeno do Alto Juruá, Estado do Acre, Brasil.* 167 pp. Unpublished M.Sc. Thesis, Universidade Federal do Rio Grande do Sul, Porto Alegre.

Schroeder, A.B., Dobson, E.T.A., Rueden, C.T., Tomancak, P., Jug, F., and Eliceiri K.W. 2021. The ImageJ ecosystem: Open-source software for image visualization, processing, and analysis. *Protein Science* 30: 234–249.

Silva, M.N. and Negri, F.R. 2016. *Sítio Fossilífero Morro do Careca (Formação Solimões), Tarauacá, Acre: sistemática e diversidade* [available online, https://www.sbpcnet.org.br/livro/68ra/resumos/resumos/4414_139fabfafb7a0faf925aa189df46b6c99.pdf].

Skandalos, P. and Van Den Hoek Ostende, L.W. 2023. Wear-dependent molar morphology in hypsodont rodents: The case of the spalacine *Pliospalax*. *Palaeontologia Electronica* 26 (3): a47.

Solórzano, A., Encinas, A., Kramarz, A., Carrasco, G., Montoya-Sanhueza, G., and Bobe R. 2021. Late early Miocene mammals from Laguna del Laja, Cura-Mallín Formation, south-central Chile (~37°S) and their biogeographical and paleoenvironmental significance. *Journal of South American Earth Science* 112 (1): 103544.

Souza-Filho, J.P., Guilherme, E., Toledo, P.M., Carvalho, I.S., Negri, F.R., Maciente, A.A.R., Cidade, G.M., Lacerda, M.B.S., and Souza, L.G.

2020. On a new *Melanosuchus* species (Alligatoroidea: Caimaninae) from Solimões Formation (Eocene–Pliocene), northern Brazil, and evolution of Caimaninae. *Zootaxa* 4894: 561–593.

Stutz, N.S., Abello, M.A., Marivaux, L., Boivin, M., Pujos, F., Benites-Palomino, A.M., Salas-Gismondi, R., Tejada-Lara, J.V., Andriolli Custódio, M., Roddaz, M., Ventura Santos, R., Ribeiro, A.M., and Antoine, P.-O. 2022. Late middle Miocene Metatheria (Mammalia: Didelphimorphia and Paucituberculata) from Juan Guerra, San Martín Department, Peruvian Amazonia. *Journal of South American Earth Sciences* 118: 103902.

Stutz, N.S., Hadler, P., Negri, F.R., Marivaux, L., Antoine, P.-O., Pujos, F., Jacó, T.R., Fontoura, E.M., Kerber, L., Hsiou, A.S., Santos, R.V., Alvim, A.M.V., and Ribeiro, A.M. 2023. New records of marsupials from the Miocene of Western Amazonia, Acre, Brazil. *Acta Palaeontologica Polonica* 68: 457–475.

Stutz, N.S., Ribeiro, A.M., Charruault, A.-L., Boivin, M., Pujos, F., Salas-Gismondi, R., Tejada-Lara, J.V., Benites-Palomino, A.M., Orliac, M.J., Varas-Malca, R., Marivaux, L., and Antoine P.-O. 2026. Hidden diversity of Palaeogene metatherians: a new family of polydolopimorphian marsupials from Peruvian Amazonia. *Zoological Journal of the Linnean Society* 206 (4): zlag006.

Tejada-Lara, J., Salas-Gismondi, R., Pujos, F., Baby, P., Benammi, M., Brusset, S., De Franceschi, D., Espurt, N., Urbina, M., and Antoine, P-O. 2015. Life in protoamazonia: Middle Miocene mammals from the Fitzcarrald Arch (Peruvian Amazonia). *Palaeontology* 58: 341–378.

Upham, N.S. and Patterson, B.D. 2012. Diversification and biogeography of the Neotropical caviomorph lineage Octodontoidea (Rodentia: Hystricognathi). *Molecular Phylogenetics and Evolution* 63: 417–429.

Upham, N.S. and Patterson, B.D. 2015. Evolution of caviomorph rodents: a complete phylogeny and timetree for living genera. *In*: A.I. Vassallo and D. Antenucci (eds.), *Biology of Caviomorph Rodents: Diversity and Evolution*, 63–120. Sociedad Argentina para el estudio de los Mamíferos (SAREM), Buenos Aires.

Upham, N.S., Ojala-Barbour, R., Brito, J.M., Velazco, P.M., and Patterson, B.D. 2013. Transitions between Andean and Amazonian centers of endemism in the radiation of some arboreal rodents. *BMC Evolutionary Biology* 13: art. 191.

Urrea-Barreto, F.J., Link, A., Carrillo, J.D., Vanegas, A., Perdomo, C., Cooke, S.B., Tallman, M., and Pérez, M.E. 2023. Systematic revision of *Neoreomys huilensis* Fields (Rodentia, Hystricognathi) from the Middle Miocene of La Venta (Villavieja, Huila, Colombia). *Geodiversitas* 45: 721–737.

Verzi, D.H., Morgan, C.C., and Olivares, A.I. 2015. The history of South American octodontoid rodents and its contribution to evolutionary generalisations. *In*: F.G. Cox and L. Hautier (eds.), *Evolution of the Rodents. Advances in Phylogeny, Functional Morphology and Development*, 139–163. Cambridge University Press, Cambridge.

Verzi, D.H., Olivares, A.I., and Morgan, C.C. 2013. Phylogeny and evolutionary patterns of South American octodontoid rodents. *Acta Palaeontologica Polonica* 59: 757–769.

Verzi, D.H., Olivares, A.I., Morgan, C.C., and Alvarez, A. 2016. Contrasting phylogenetic and diversity patterns in octodontoid rodents and a new definition of the family Abrocomidae. *Journal of Mammalian Evolution* 23: 93–115.

Vitek, N.S. and Chen, H. 2022. The impact of tooth wear on occlusal shape and the identification of fossils of New World Porcupines (Rodentia: Erethizontidae). *Journal of Mammalian Evolution* 29: 677–692.

Voss, R.S., Hubbard, C., and Jansa, S.A. 2013. Phylogenetic Relationships of New World Porcupines (Rodentia, Erethizontidae): Implications for Taxonomy, Morphological Evolution, and Biogeography. *American Museum Novitates* 2013 (3769): 1–36.

Vucetich, M.G. 1984. Los roedores de la Edad Friasense (Mioceno Medio) de Patagonia *Revista del Museo de La Plata: (Nueva Serie). Sección Paleontología* 50: 47–126.

Vucetich, M.G. and Bond, M. 1984. Un nuevo Octodontoidea (Rodentia, Caviomorpha) del Oligoceno tardio de la Provincia de Chubut (Argentina). *Ameghiniana* 21: 105–114.

Vucetich, M.G. and Kramarz, A.G. 2003. New Miocene rodents from Patagonia (Argentina) and their bearing on the early radiation of the octodontoids (Hystricognathi*). Journal of Vertebrate Paleontology* 23: 435–444.

Vucetich, M.G., Arnal, M., Deschamps, C.M., Pérez, M.E., and Vieytes, E.C. 2015. A brief history of caviomorph rodents as told by the fossil record. *In*: A.I. Vassallo and D. Antenucci (eds.), *Biology of Caviomorph Rodents: Diversity and Evolution*, 11–62. Sociedad Argentina para el estudio de los Mamíferos (SAREM), Buenos Aires.

Vucetich, M.G., Carlini, A.A., Aguilera, O., and Sánchez-Villagra, M.R. 2010a. The tropics as reservoir of otherwise extinct mammals: The case of rodents from a new Pliocene faunal assemblage from Northern Venezuela. *Journal of Mammalian Evolution* 17: 265–273.

Vucetich, M.G., Deschamps, C.M., and Pérez, M.E. 2012. Palaeontology, evolution and systematics of capybaras. *In*: J.R. Moreira, K.M.P.M. de Barros Ferraz, E.A. Herrera, and D.W. Macdonald (eds.), *Capybara: Biology, Use and Conservation of an Exceptional Neotropical Species*, 39–59. Springer, New York.

Vucetich, M.G., Deschamps, C.M., Olivares, A.I., and Dozo, M.T. 2005. Capybaras, shape, size and time: a model kit. *Acta Palaeontologica Polonica* 50: 259–272.

Vucetich, M.G., Kramarz, A.G., and Candela, A.M. 2010b. Colhuehuapian rodents from Gran Barranca and other Patagonian localities: the state of the art. *In*: R.H. Madden, A.A. Carlini, M.G. Vucetich, and R.F. Kay (eds.), *The Paleontology of Gran Barranca, Evolution and Environmental Change through the Middle Cenozoic of Patagonia*, 206–219. Cambridge University Press, Cambridge.

Vucetich, M.G., Mazzoni, M.M., and Pardiñas, U.F.J. 1993. Los roedores de la Formación Collón Curá (Mioceno Medio), y la ignimbrita Pilcaniyeu. Cañadón del Tordillo, Neuquén. *Ameghiniana* 30: 361–381.

Walton, A.H. 1990. *Rodents of the La Venta Fauna, Miocene, Colombia: Biostratigraphy and Paleoenvironmental Implications.* 153 pp. Unpublished Ph.D. Thesis, Southern Methodist University, Dallas.

Walton, A.H. 1997. Rodents. *In*: R.F. Kay, R.H. Madden, R.L. Cifelli, and J.J. Flynn (eds.), *Vertebrate Paleontology in the Neotropics. The Miocene Fauna of La Venta, Colombia*, 392–409. Smithsonian Institution Press, Washington.

Wilson, D.E., Lacher, T.E., and Mittermeier, R.A. 2016. *Handbook of the Mammals of the World. Vol. 6. Lagomorphs and Rodents*. 987 pp. Lynx Edicions, Barcelona.

Wood, A.E. 1955. A revised classification of the rodents. *Journal of Mammalogy* 36: 165–187.

Wood, A.E. and Patterson, B. 1959. The rodents of the Deseadan Oligocene of Patagonia and the beginnings of South American rodent evolution. *Bulletin of the American Museum of Natural History* 120: 279–428.

Woods, C.A., and Kilpatrick, C.W. 2005. Infraorder Hystricognathi. *In:* D.E. Wilson and D.M. Reeder (eds.), *Mammal Species of the World: A Taxonomic and Geographic Reference, 3rd edition*, 1538–1600. Johns Hopkins University Press, Baltimore.